European Cells and Materials Vol. 1. Suppl. 1, 2001 (pages 3-4) ISSN 1473-2262

# DEVELOPMENT OF A TEXTILE WOUND DRESSING BASED ON EMBROIDERY TECHNOLOGY

Erdal Karamuk[1], Mario Billia[2], Bernhard Bischoff[3], Renato Ferrario[3], Bärbel Wagner[4], René Moser[5], Marcus Wanner[6] and Jörg Mayer[1]

*[1]Biocompatible Materials Science and Engineering, ETH, Zürich, Switzerland, [2] TISSUPOR AG, St. Gallen, Switzerland, [3]Bischoff Textil AG, St. Gallen, Switzerland, [4]Swiss Federal Laboratories for Materials Testing and Research (EMPA), St. Gallen, Switzerland, [5]Institute for Biopharmaceutical Research (IBR)-Inc, Matzingen, Switzerland, [6]Swiss Paraplegics Center (SPZ), Nottwil, Switzerland*

**INTRODUCTION:** Non healing wounds have a great economic impact because they need intensive wound care for very long periods, often disabling the patient and causing high health care costs. One of the key issues in tissue regeneration of chronically non healing wounds is controlled revascularisation of the epidermal tissue. In textile implant materials tissue formation and vascularisation depend on the size and distribution of pores and fibers[1]. An arrangement of pores of different orders of magnitude will favour the tissue ingrowth and the formation of new blood wessels and capillaries[1]. We developed a new textile wound dressing based on embroidery for the treatment of chronically non healing wounds (TISSUPOR®). Embroidery technology allowed to achieve a 3-dimensionally structured textile architecture that combines pores for directed angiogenesis and elements for local mechanical stimulation of the wound ground[2] (fig. 1).

**METHODS:** The adaptation of the industrial embroidery process to medical textiles requires thorough biocompatibility testing to find possible toxic effects of chemical residues from machine, base cloth or yarn sizing. We performed cytotoxicity assays using a 3T3 fibroblast cell line. In direct and indirect (using extracts) exposure methods, endpoints and time course of mitochondric activity (MTT) and cell mass (DNA / direct counting) were measured. In both cases no significant toxic effects were detected.
Clinical pilot studies were initiated, focussing on the treatment of venous leg ulcers (ulcus cruris) and pressure soars (decubitus). Decubitus was treated at the wound care clinic at the SPZN under according to SPZ protocols. Wounds were treated with TISSUPOR® after initial debridement until 50 % wound surface reduction.

**RESULTS:** First results show a comparable healing rate to conventional moist wound care. A high induction of granulation tissue was observed, especially in deep (wound volume >80ml, fig. 2) and infected wounds.

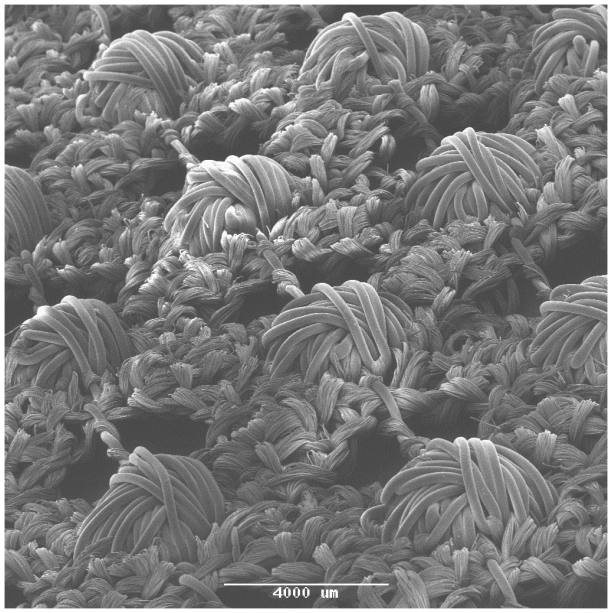


*Fig. 1: SEM image of the embroidered textile layer of the wound dressing. The porous structure is made from PET multifilament yarns, whereas the stiff elements for mechanical stimulation consist of PA monofilaments.*

*Fig. 2: Example of wound treatment with TISSUPOR®: Female patient, age 69, inidaction decubitus. Wound volume after one week was 80ml. Dressing was changed twice a week. After 2 weeks the wound volume was 40 ml (left) The wound was surgically closed after 3.5 weeks of application, when the wound volume was 11ml (right).*

**DISCUSSION & CONCLUSIONS:** The application concept of TISSUPOR® which is based on the working hypothesis that bleeding must be induced when changing the wound dressing to reactivate the wound healing by creating an acute inflammative raction resulted in much less frequent dressing changement (2 times per week instead of twice a day) which seems promising for a commercial success both in clinical and ambulant treatment of chronic wounds. A european wide multicenter study was initiated for the treatment of chronic wounds with a wide range of indications.

**REFERENCES:** [1]E. Wintermantel, et al. (1992), in: Angiogenesis: Principles - Science - Technology - Medicine. [2] E. Karamuk et al. (1999) in S. Anand ed *Medical Textiles '99*,. Woodhead, UK, in press.

**ACKNOWLEDGEMENTS:** This study was supported by the KTI - MedTech Initiative of the Swiss Federal Office for Professional Education and Technology.

# DEGRADATION OF AN EXPERIMENTAL CALCIUM-PHOSPHATE CEMENT IN A SHEEP MODEL

A. Gisep[1], R. Wieling[1], M. Bohner[2], S. Matter[3], E. Schneider[1], B. Rahn[1]

[1] AO Research Institute, Clavadelerstrasse, CH-7270 Davos Platz, [2] RMS Foundation, Bischmattstrasse 12, CH-2544 Bettlach, [3] STRATEC Medical, Eimattstrasse 3, CH-4436 Oberdorf

**INTRODUCTION:** In orthopaedic surgery, reconstruction of bone defects – be it after tumour resection or comminuted articular fractures – is still a challenging problem. The use of autologous bone as a filler material for these voids is known as the golden standard. However, there are problems like limited availability and donor site morbidity which led to the use of allografts or the development of synthetic bone graft materials. For more than 100 year already, different materials such as coral or gypsum have been implanted. Among these, the calcium-sulphates were the first ones that hardened in situ and proved their potential as bone substitute materials. Later, different types of calcium-phosphate cements (CPC) were introduced. Various CPCs are currently commercially available, whereas others are still in an experimental phase. One of these experimental cements consists of two phases: a brushite matrix with β-TCP granules in it. This should lead to a different degradation pattern as compared to the monophasic apatite-cements. This study investigated the in vivo degradation patterns of experimental biphasic CPCs and the concomitant bone remodelling processes in a sheep model.

**MATERIALS AND METHODS:** As implant materials, 2 different Ca-P cements were used: an experimental biphasic material consisting of a brushite matrix ($CaHPO_4 \cdot 2H_2O$; DCPD) and β-tricalcium-phosphate ($Ca_3(PO_4)_2$; β-TCP) granules which are embedded in the matrix after the hardening process. As a comparison to this experimental cement, a monophasic hydroxyapatite cement ($Ca_5(HPO_4)_3OH$; HA) was implanted.

As an animal model, the canine model published by Frankenburg et al.* was adapted to the Swiss Mountain Sheep (animal permit GR 01/2000). The following defects were created: a) a slot defect with a heigth of 6 mm to the proximal tibial metaphysis, 10 mm below the articular surface. It penetrated the tibial head to 50% of its depth, leaving the posterior cortex intact;

b) in both femoral condyles, a drill hole (8 mm diameter and 16 mm) depth was created. All defects were filled with the ceramic bone cements.

Post operative x-rays on a weekly basis and clinical observation was done to ensure the sheep's healthy status. The animals were sacrificed 8 and 20 weeks. After harvesting of bone specimens, histologic processing included embedding in polymethylmethacrylate, 200 µm sectioning (Leitz Saw Microtome 1600), grinding (Exact) and surface staining (Giemsa-Eosin). Microscopic analysis and digital imaging was done to evaluate cement resorption and bone remodelling.

**RESULTS:** In the biphasic cement, the brushite matrix was resorbed faster than the β-TCP granules. This resulted in free granules which were used by newly growing bone as a guidance. Bone filled most of the spaces which were left from the degrading cement. The granules acted as a "negative scaffold". There was intimate contact from new grown bone to the implant material, indicating good biocompatibility of the cement. The new cancellous bone showed a 3-D structure.

An unexpected effect was the accelerated resorption of β-TCP granules once they were no more totally surrounded by DCPD matrix. This could be due to the fact that the porosity of the granules was higher as compared to the matrix. The granules mostly showed faster resorption in their centre. After advanced resorption, the granules got incorporated into the formation of new bone, lamellar structures also growing through the TCP granules. This points to a bone remodelling process that follows the regional demands more than the "negative scaffold effect".

The monophasic HA-cement showed slower resorption in all defects. There always was a very close contact between bone and implant material, again revealing a good compatibility. Resorption only occurs on the surface of the implant. All cracks and pores in the cement were filled with bone or osteons.

All these effects were observed in all tibial and femoral defects, regardless of the loading situations occurring at the specific site.

**CONCLUSIONS:** The degradation patterns of both types of cements, monophasic and biphasic, seem to allow for a continuous load bearing function during their replacement by bone. According to the required duration of function and the expected loading situation, the monophasic HA-, or the more rapidly degrading biphasic DCPD/β-TCP-cement may be chosen.

**REFERENCES:** *Frankenburg et al. (1998) JBJS Am, 80-8, 1112 - 1124

# ASSESSMENT OF PHYSICAL PROPERTIES OF TISSUES AND BONE SUBSTITUTES MATERIALS IN HISTOLOGIC SECTIONS BY SCANNING ACOUSTIC MICROSCOPY (SAM)

L. Feuz[1,2], A. Gisep[2], P. Pyk[2], B. Rahn[2]

[1] *Institute for Nonmetallic Inorganic Materials, ETH Zurich, Switzerland,*
[2] *AO Research Institute, Davos, Switzerland*

**INTRODUCTION:** Large bone loss is mostly treated by autologous bone transplantation. Bone substitutes such as calcium phosphates (Ca-P) have been developed to enhance the healing process in cases where the amount of bone available is not sufficient to reconstruct the injured part. The assessment of mechanical property changes of these *in vivo* degrading materials and their gradual replacement by bone is of great practical importance. Scanning Acoustic Microscopy (SAM) is a non-destructive method, which works on the principle of propagation and reflection of acoustic waves at interfaces and is able to provide information about local density and stiffness with a lateral resolution of a few tenths of microns.[1] The aim of this study is to set up a SAM measurement system that permits characterization of histologic specimens with an additional focus on their mechanical properties. Aspects like sample preparation and long-term stability of the measurements are discussed since high resolution scans are of extremely long duration.

**METHODS:** The Scanning Acoustic Microscope used in this study works in reflection mode and is operated at 50 MHz in a pulse mode (Fig. 1, left). Using the time difference between the upper and lower surface reflection signal (Fig. 1, right), ultrasonic wave velocity can be calculated. This parameter together with acoustic impedance is used to calculate density and modulus. Experiments were performed on histologic samples (embedding medium poly (methyl methacrylate) with different tissues (bone, Ca-P cement, dentine, enamel, soft tissues). The effect of sample preparation on SAM measurements was investigated. Milled and additionally polished samples were used.

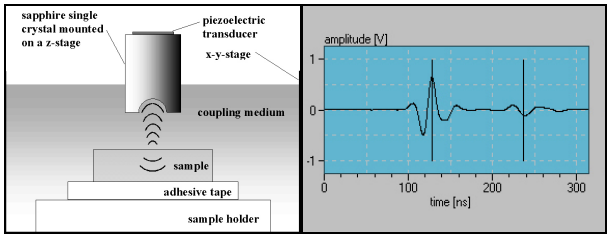


*Fig. 1: left, the SAM setup; right, measurement of ultrasonic wave velocity: the first signal stems from the upper, the second from the lower surface reflection.*

Samples were measured in different coupling media for 48 hours with SAM. Among the screened media distilled water and a 0.1 M phosphate buffer solution (PBS) at pH 7.4 are currently under detailed investigation. Laser profilometry has been performed to characterize the surface roughness ($R_a$, $R_{z(DIN)}$).

**RESULTS:** The reflected signal in SAM measurements is 5-15 % stronger for the polished sample and surface roughness decreases with additional polishing. A correlation between surface roughness and reflection behavior of the sample can be presumed. Concerning coupling media, water based solutions permit a good signal transmission whereas paraffin oil and glycerin did not allow good wave propagation. So far, different tissues like cement, bone, connective tissue, dentine and enamel could be distinguished unambiguously with respect to impedance, velocity, density and modulus. In the long-term measurements a decrease in impedance of 2-12 % has been measured after 48 hours for both systems ($H_2O$, PBS). Surface roughness showed a significant increase during this time so that dissolution or deposition processes on the sample surface could be supposed.

**DISCUSSION & CONCLUSIONS:** Scanning Acoustic Microscopy seems to be a helpful tool to analyze histologic sections in addition to fluorescence microscopy, polarized light microscopy and surface staining for cellular details. Information about mechanical properties can be precisely associated with a topographic location. The operating frequency of 50 MHz allows investigations with a resolution of 30 µm of both surface and bulk properties, which is a particular feature of this microscope. However, the absolute values measured must be interpreted with caution, since sample preparation affects the reflection behavior of the sample. Therefore, the method appears to be useful for comparative analysis of samples with the same preparation history. The results have to be calibrated with other established methods.

**REFERENCE:** [1] A. Briggs (1992) *Acoustic Microscopy*, Clarendon Press, Oxford.

European Cells and Materials Vol. 1. Suppl. 1, 2001 (pages 7-8) ISSN 1473-2262

# HIGH LOAD BEARING, HIGH RELIABLE ALL-CERAMIC DENTAL BRIDGES BY THE DIRECT CERAMIC MACHINING PROCESS

F. Filser[1], H. Lüthy[2], P. Kocher[1], P. Schärer[2], and L.J. Gauckler[1]

[1]*Nonmetallic Inorganic Materials, Dept. of Materials, Swiss Federal Institute of Technology, Zurich, Switzerland,* [2]*Center for Dental and Oral Medicine, University of Zurich, Switzerland*

**INTRODUCTION:** All-ceramic dental bridges are highly desired as they offer the advantages of a metalfree treatment. Due to the weak mechanical properties of traditional dental ceramics ceramic bridges have to be designed up to now with thick connectors (about 16 to 20 mm$^2$) for bearing the mastication loads in the posterior region (880 N). Zirconia in its tetragonal yttria stabilized polycrystal form (TZP) offers highest strength combined with highest toughness. However, TZP is difficult to machine in its dense state and has therefore found only limited application for dental bridges. A new Direct Ceramic Machining (DCM) process uses porous, easy-to-machine TZP blanks and machines the frameworks in an enlarged shape to compensate for the sintering shrinkage. We compare the load bearing and reliability of frameworks and bridges fabricated by the DCM process to other dental ceramic materials and evaluated their failure probability.

**METHODS:** The fabrication of frameworks via the DCM process route starts with the acquisition of the framework model's surface (fig.1) [1]. The data is linearly enlarged by about 50 vol-%, tool path information is generated for the machine and then the TZP blank is milled. The yet porous, enlarged framework is sintered to full density and at the same time shrinks to its final dimension. Veneer porcelain layers are fired on the TZP framework to complete the bridge. Frameworks and bridges with 6.9 mm$^2$ connector area were mechanically tested (fig.2). The test setup was designed to produce failures of clinical relevance. The TZP specimens were fabricated by DCM and compared to similar shaped specimens made of glass-ceramics (IPS Empress2) and of glass-infiltrated alumina material (In-Ceram Alumina) fabricated according to manufacturers' instructions. Load bearing was recorded, and Weibull statistic was used to determine reliability and failure probability.

**RESULTS:** The TZP frameworks and bridges show the highest load bearing of all investigated ceramics (fig.3). We also found the highest reliability e.g. the lowest scattering of load bearing values for the DCM fabricated frameworks and bridges. The failure probability of the TZP bridges for 880 N is about 2 percent, whereas all other ceramic bridges would fracture to 100 %.

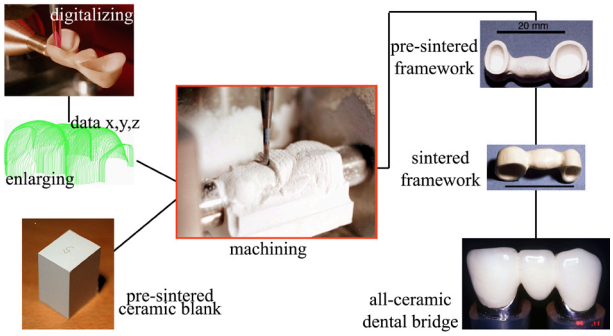


*Fig. 1: Direct Ceramic Machining Process.*

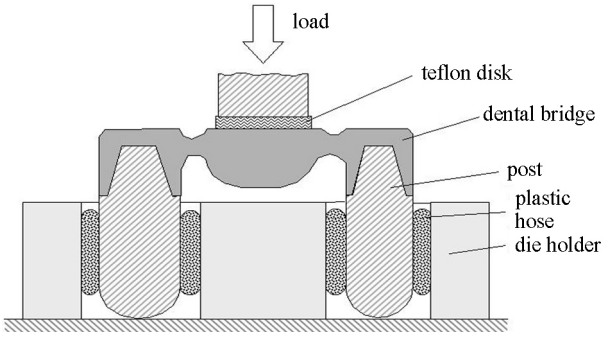


*Fig. 2: Test setup for load bearing.*


*Fig. 3: Fracture of a framework in the connector.*

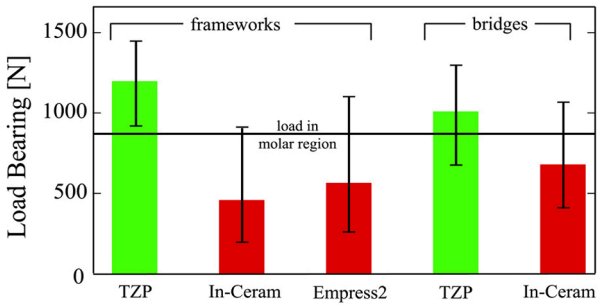


*Fig. 3: Load bearing of frameworks and bridges.*

*Table 1. Reliability is represented by Weibull moduli.*

| | Framework | Bridge |
|---|---|---|
| TZP | 8.5 | 6.1 |
| Glass-infiltrated Alumina | 2.7 | 3.6 |
| Glass-Ceramic | 3.0 | - |

**DISCUSSION & CONCLUSIONS:** DCM fabricated TZP bridges bear reliably highest mastication loads in the posterior region even when using a desired gracile connector design. Therefore, we recommended TZP bridges for clinical use in the complete denture.

**REFERENCES:** [1] F. Filser et al. (1998) *All-Ceramic Dental Bridges by Direct Ceramic Machining (DCM)* in: *Materials in Medicine*, Eds. M.O. Speidel et al.: vdf Hochschulverlag, ETH Zurich: Zurich. p. 165-189.

**ACKNOWLEDGEMENTS:** This work was supported by the Swiss Priority Program for Materials Research.

European Cells and Materials Vol. 1. Suppl. 1, 2001 (pages 9-10) ISSN 1473-2262

# SELF-ASSEMBLED MONOLAYERS OF ALKANEPHOSPHATES ON TITANIUM OXIDE SURFACES

S.Tosatti, R. Hofer, M. Textor and N.D. Spencer

*Laboratory for Surface Science and Technology ,Departement of Materials, ETH Zürich,CH-8092 Zürich, Switzerland*

**INTRODUCTION:** Self-assembled monolayers of thiols on gold surfaces are widely used to produce model surfaces with well-defined chemical composition for a variety of applications including biomaterial and biosensor surfaces [1,2]. Alkane-phosphates and -phosphonates have been shown to form SAMs on a number of transition metal oxide surfaces such as titanium oxide ($TiO_2$), tantalum oxide ($Ta_2O_5$) and niobium oxide ($Nb_2O_5$) [3,4]. Using a combination of dedicated surface characterization techniques, the molecular structure of these adlayers has been demonstrated to be similar to thiols on gold with an intermolecular spacing of 5 Å (corresponding to 21 $Å^2$ per molecule) and a tilt angle of the molecular axis of 30–35° relative to the surface normal (Fig. 1). The binding of the phosphate head group to the metal oxide surface is believed to be through direct coordination between phosphate and metal cation and arguments have been given for the presence of both mono- and bi-dentate binding of the phosphate group thus enabling the formation of a close-packed layer.

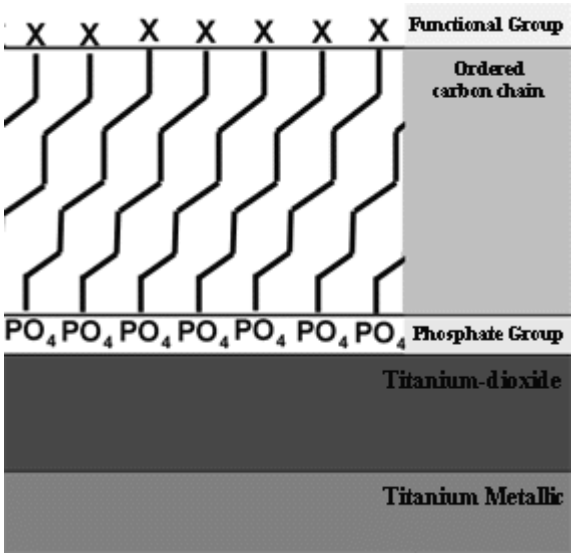


*Fig. 1: Self-assembled monolayer of X-functionalized alkane phosphate on a titanium (oxide) surface*

The use organic solvent solution to produce surface layers has clear disadvantages if the perspective is to use such techniques on an industrial scale. Moreover, for applications in areas such as medical devices and implants, the presence of even minor organic solvent residues in the adlayers may not be tolerated in view of potential cell-toxic effects and other biological risks. Therefore, a technique based on the deposition of SAMs from water-soluble alkylphosphate solutions has been developed and successfully applied to a variety of metal oxide substrates [5].

This paper descibes the application of methyl-terminated ("non-functionalized") and hydroxy-terminated dodecylphosphates ($DDPO_4$ and OH-$DDPO_4$ resp.) on flat/smooth titanium or titanium-oxide coated substrates as well as on rough (grit-blasted and acid-etched) titanium surfaces.

**METHODS:**

*Substrates:* Three different substrates were used: a) thin film of titanium dioxide ($TiO_2$) (20 nm) and b) titanium metal (100 nm) resp. deposited by physical vapor (PSI Villigen) onto silicon wafers or flat glass slides. c) Commercially pure (CP) titanium discs were grit-blasted and subsequently etched (received from Institut Straumann AG, Waldenburg).

*Alkanephosphates and SAM formation:* The used alkyl-phosphates molecules were prepared according to a previous publication [4,5]. The substrates were solvent cleaned and immersed for 48 hours in the aqueous amphiphile solution. The alkyl-phosphate and hydroxyalkyl-phosphate solutions were mixed in different ratios from 0 to 100 vol.-% with respect to the amount of OH-$DDPO_4(NH_4)_2$ at constant total phosphate concentration of 0.5 mM.

*Contact angle Measurement:* Surface wettability was investigated trough measuring advancing and receeding contact angle in a sessile water drop type of experiment. The measurements were performed in an automated way by stepwise increasing and decreasing respectively the water drop size.

**RESULTS:** Fig. 2 and 3 show the advancing and receeding contact angles of smooth titanium oxide surfaces and of structured SLA surfaces resp. after formation of a self-assembled monolayer from mixed aqueous solution of $DDPO_4$/OH-DDP $O_4$.

The contact angles depend on both the surface chemistry (composition of SAM) and the topography of the surface.

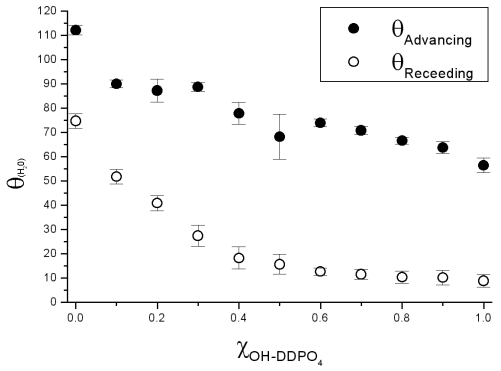


*Fig. 2: Advancing and receeding contact angles of water on smooth titanium metal coated silicon wafer surfaces as a function of the the OH-$DDPO_4(NH_4)_2$ concentration in the SAM forming solution, expressed as the mole fraction $\chi_{OH\text{-}DDP04}$*

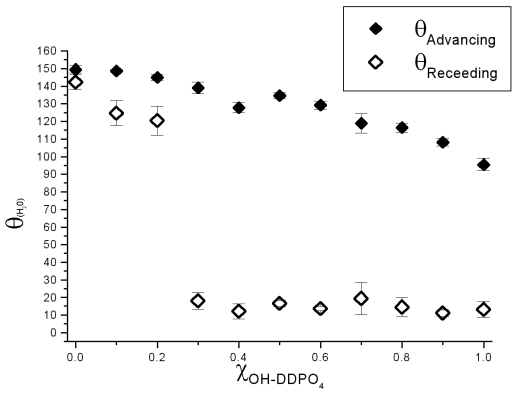


*Fig. 3: Advancing and receeding contact angles of water on rough, particle blasted and acid etched (SLA) titanium metal surfaces as a function of he OH-$DDPO_4(NH_4)_2$ concentration in the SAM forming solution, expressed as the mole fraction $\chi_{OH\text{-}DDP04}$*

The comparison between the experimental contact angles and model calculation based on equations given by Cassie [6] and by Israelatchvili and Gee [7] as well as detiled XPS analysis give evidence that the OH-$DDPO_4$ adsorbs somewhat preferentially leading to a ratio of OH-$DDPO_4$/$DDPO_4$ in the adlayer that is typically a factor of 1.4 higher than expected from the molar ratio in the aqueous amphiphile solution.

**DISCUSSION & CONCLUSIONS:** Alkanephosphates can be self-assembled from aqueous solution on titanium oxide surfaces to produce model surfaces with very well-controlled surface properties such as wettability. The technique is suitable to modify both flat/smooth surfaces and rough, highly structures surfaces. Such surfaces may have applications in the area of optical waveguide sensors (where transparent oxide-covered chips are used) and as model surfaces for cell–surface interactions. In the latter case, the possibility of independent control over the surface chemistry and the topography makes such systems particularly attractive for basic studies.

**REFERENCES:**

[1]Bain, C. D. et al.; J. Am. Chem. Soc.; 111; 321; (1989)

[2]Nuzzo, R.; Allara, D. L.; J. Am. Chem. Soc., 105; 4481-4483; (1983)

[3]Brovelli, D. et al.; Langmuir; 15; 4324-4327; (1999)

[4]Textor, M. et al.; Langmuir; 16; 3257-3271; (2000)

[5]Hofer, R.; Textor, M.; Spencer, N. D.; Submitted to Langmuir; (2001)

[6]Cassie, A. B. D.; Discuss. Faraday Soc.; 4; 5041; (1952)

[7]Israelachvili, J. N.; Gee, M. L.; Langmuir; 5; 288-289; (1989)

**ACKNOWLEDGEMENTS:** Financial support by ITI Research Foundation, Waldenburg and technical support by Institut Straumann AG, Waldenburg is acknowledged.

# MICROPATTERNS OF FUNCTIONAL PROTEINS FOR CELL CULTURES

L. Tiefenauer, H. Sorribas and C. Padeste

*Paul Scherrer Institut, 5232 Villigen PSI, Switzerland*

**INTRODUCTION:** The importance of topological and chemical surface structures on the behaviour and the functionality of cultured cells is well recognised. Various cell types, however, react differently and little is known about the *specific* reactions of most cell types. For a more detailed investigation on the interaction of cells with structured surfaces micropatterns of specific proteins have been developed.

Adhesion proteins are especially interesting for cell-surface investigations. Gene constructs of the chicken neuron membrane proteins axonin-1 and NgCAM have been generated wherein the transmembrane part has been replaced by a sequence encoding for a peptide-linker ending with a C-terminal cysteine [1]. The thiol-group of Cys permits a stable immobilisation of the recombinant adhesion proteins directly on gold surfaces or alternatively on other materials, which have previously been functionalised with maleinimid-groups.

**METHODS:** In order to achieve a stable immobilisation, glass surfaces were first silanised and by using heterobifunctional crosslinkers the recombinant proteins were covalently attached. Standard positive photoresist techniques were adapted to generate micropatterns of proteins on glass. Both lift-off and plasma etching techniques were used to transfer the photoresist pattern into a layer of the covalently immobilised peptides or protein. Fragile proteins such as the mentioned adhesion proteins have to be protected by a thin sucrose layer in a first step. By a combination of the lift-off and the etching technique complementary patterns of two different proteins were generated.

**RESULTS:** Neurons were cultured on the unstructured chips and we observed six times longer neural outgrowths on NgCAM than on aminosilane, whereas on axonin-1 the mean lengths increased only by a factor of two [2]. This result shows that the adherence of cells strongly depends on the surface chemistry and that immobilised adhesion proteins specifically induce cellular reactions. We didn't observe a decrease in the biological activity of the immobilised proteins during several weeks.

By using the microstructuring techniques grids of axonin-1 were produced on glass chips. In cultures of dissociated neurons from chicken dorsal root ganglia the cells preferentially adsorb to the knots in the grid. Their neural outgrowths spontaneously align along the protein lines. Thus, micropatterns of specific adhesion proteins are useful to establish neuronal networks. Furthermore, arrays of gold microelectrodes have been produced, which allow us to address individual cells. The preliminary electrophysiological measurements look promising. When specific adhesion proteins are present on electrodes the neuron-electrode contact may be improved as measurements of the mean distance of the cell membrane to the material surface indicate [1].

When micropatterns of two different proteins are generated on one surface, a resolution of 2 μm could be achieved. The functionality of the two proteins streptavidin and IgG has been tested using fluorescence microscopy: the areas where the added biotin-fluorescein conjugate was bound appeared in green, the IgG areas with the bound second-antibody-rhodamine-conjugate were red.

**DISCUSSION & CONCLUSIONS:** The techniques described here have a high potential for more general applications in biomaterials research. The generation of specific protein patterns allows us to establish co-cultures of two different cell types. Recently, it became evident that glia cells play a more active role in synapsogenesis than previously assumed [3]. It can be assumed that a close contact of two different cell types is also important for many further complex biological processes. Thus, co-cultures on predefined microstructured patterns may play a key role in the future research of biomaterials.

**REFERENCES:** [1] H. Sorribas, D. Braun, L. Leder, P. Sonderegger and L. Tiefenauer (2001) *J. Neurosci. Meth.* **104**:133-141. [2] H. Sorribas, C. Padeste, T. Mezzacasa and L. Tiefenauer (1999) *J. Mater. Sci.: Mater. Med.* **10**:787-791. [3] E. Ullian, S. Sapperstein, L. Christopherson and B. Barres (2001) Science **291**:657-660.

**ACKNOWLEDGEMENTS:** This work has been supported by the Swiss Priority Program Biotechnology, module Neuroinformatics, project No. 5002-44890. We acknowledge the contribution and support of P. Sonderegger, University of Zürich, and of L. Leder, Novartis AG, Basel.

European Cells and Materials Vol. 1. Suppl. 1, 2001 (pages 12-13) ISSN 1473-2262

# Enhancement of immunogold labelled vinculin in cells cultured on metal implant surfaces

G.Rh.Owen[1], D.O. Meredith [1], I. ap Gwynn [2], and R.G. Richards[1]

[1]Interface Biology, AO Research Institute, Clavadelerstrasse, CH-7270 Davos Platz, Switzerland
[2]Institute of Biological Sciences, The University of Wales, Aberystwyth, Wales, GB.

INTRODUCTION: Cells adhere onto proteins adsorbed on implant materials by focal adhesions. The focal adhesion is a complex of integrin transmembrane receptors associated indirectly with the actin cytoskeleton by linker proteins. One important linker protein stabilising the entire focal adhesion structure is vinculin. The area of focal adhesions is known to correlate with adhesion strength and has been used as a method to determine the cytocompatibility of implant materials (1-2). Many techniques have been used to label the focal adhesions with the objective of measuring the total area of adhesion on different materials. Limitations to the specificity and resolution of these labels have proven to be problematic and consequently results are highly variable. A specific label, utilising ultrasmall gold particles attached to secondary antibodies, made it possible to localise individual antigens at high resolution with an electron microscope (3). Immunogold labelling with small probes has not been successful, to date, when labelling cells on metal substrates. Enlarging these probes with a silver solution is necessary to image them with a scanning electron microscope (SEM). However, heavy metal stains such as osmium tetroxide etch the enhanced particles reducing them to approximately their original size. High concentrations of osmium are used to provide sufficient electron density to the cell for imaging on the metal substrate. One method to protect the silver is by plating the silver with gold. Gold plating (toning) however replaces the outer silver shell with several gold particles therefore quantification is not possible since, stoichiometrically, the number of gold particles do not reflect the number of antigenic sites. Consequently a new Gold Enhance™ solution has been produced by Nanoprobes. This enhancement is resistant to the etching effects of osmium. We show that immunogold labelling on metal surfaces is possible with both silver enhancement, in the absence of osmium tetroxide, and gold enhancement in the presence of osmium. We postulate a mechanism to explain the etching of silver particles in material attached to metal surfaces.

METHODS: Fibroblasts and osteoblasts were cultured on implant quality stainless steel and tissue culture plastic for 2 days at a density of 20,000/ml. The cells were immunogold labelled for vinculin following the procedure by Richards *et al.* (submitted). Two enhancement solutions were tested. Silver enhance (British Biocell International Ltd, Cardiff, UK) and Gold enhance™ (Nanoprobes Incorporated, Yaphank, NY 11980-9710, USA). Stainless steel was used as a test substrate since it was found to be the most problematic regarding self-nucleation and non-specific background deposition of silver from the enhancing solution. The postfixation stage was varied in osmium tetroxide concentration and duration on both substrates as seen in Table 1. All samples were then dehydrated through an ethanol series, critical point dried and coated with carbon for observation with a field emission SEM.

*Table 1- Variations used in the postfixation stage of the immunogold labelling procedure. Au = gold enhance; Ag = silver enhance; M = Metal; P = Plastic; P+M = Plastic with stainless steel particles; Conc. = concentration*

| Enhance | Substrate | Osmium conc. (%) | Incubation (min) |
|---|---|---|---|
| Au | M | 1.0 | 60 |
| Ag | M | 1.0 | 60 |
| Ag | M | 1.0 | 30 |
| Ag | M | 0.1 | 60 |
| Ag | M | 0.1 | 30 |
| Ag | M | 0 | 0 |
| Au | P | 1.0 | 60 |
| Ag | P | 1.0 | 60 |
| Ag | P+M | 1.0 | 60 |

RESULTS: SEM observations have been summarised in Table 2.

*Table 2- Summary of observations from SEM images. S =spherical enhanced gold label, N=non-spherical enhanced gold label See Table 1 for other abbreviations.*

| Enhance | Substrate | Os (%) | Incubation | Labelling | Particles |
|---|---|---|---|---|---|
| Au | M | 1.0 | 60 | Yes | S |
| Ag | M | 1.0 | 60 | No | |
| Ag | M | 1.0 | 30 | Yes | S |
| Ag | M | 0.1 | 60 | Yes | S |
| Ag | M | 0.1 | 30 | Yes | S |
| Ag | M | 0 | 0 | Yes | S |
| Au | P | 1.0 | 60 | Yes | S |
| Ag | P | 1.0 | 60 | Yes | N |
| Ag | P+MP | 1.0 | 60 | No | |

DISCUSSION: Silver enhancement is a nanoscale molecular version of electroplating. Silver is plated onto the gold label in a time dependent manner. The gold label acts as a sink of electrons thereby catalysing the reduction of silver deposition onto gold. Silver is consequently plated on the gold label in a time dependent manner. GoldEnhance™ works on a principle similar to silver enhancement but its composition and formulation are not available from Nanoprobes. Silver enhanced gold particles are etched in the presence of osmium on a plastic substrate. Gold enhanced particles are not affected by osmium. Differences between silver and gold enhancing solutions can be explained by their redox potentials. The redox potential for $OsO_4$ to Os(0) (0.85V) is higher than that for Ag(I) to Ag(0) (0.96V), so the silver deposit will be oxidized by $OsO_4$, but since it has a lower potential than that for Au(I) to Au(0) (1.68V), Au(0) would not be oxidised (personal communication R. Powell, Nanoprobes). This reaction is osmium concentration and time dependent. Reducing the osmium concentration and/or time increased the observed number of labels but reducing both improved the labelling, agreeing with Bury's (4) observations.

Non-visualisation of immunogold labelling on metal substrates can be explained by the enhanced etching action of the osmium on the silver coating, catalysed by the underlying metal substrate. This is a concentration and time dependent reaction similar to the enhancing reaction.

If one is interested in immunogold labelling an antigen, in material attached to a metal surface, then the duration and concentration of osmium fixation should be scrutinised for it's effect on the silver enhancement. Where optimal osmium staining is required, it is advisable to use GoldEnhance™.

REFERENCES:

Bury, R.W. *et al* (1992) J. Histochem. Cytochem. 40: 1849-1856.

Faulk, W.P. & Taylor, G.M. (1971) Immunochemistry 8:1081-1083.

Lotz, M.M. *et al* (1989) J. Cell Biology 109: 1795-1805.

Yamamoto, A. *et al* (2000) J. Biomat. Res. 50:114-124.

European Cells and Materials Vol. 1. Suppl. 1, 2001 (pages 14-15) ISSN 1473-2262

# STABILITY AND REPASSIVATION OF METALLIC IMPLANTS IN SERUM BOVINE

F.Contu, B.Elsener, H.Böhni

*Institute for Material Chemistry and Corrosion, Swiss Federal Institute of Technology, ETH Hoenggerberg, 8093 Zurich, Switzerland*

## INTRODUCTION

Metallic implants show an outstanding corrosion resistance due to the spontaneous formation of a thin protective oxide film (the passive film) [1]. Nevertheless, clinical experience reports that a small percentage of prosthetic devices produce inflammatory response due to corrosion after insertion in the body. Fretting corrosion is regarded as the principle cause of implant failure [2, 4]. Under fretting condition, metal oxidation causes a decrease in the local pH and a rise of metal ion concentration as well as the accumulation of small metal particles. This may affect the existing balance of ions in the tissue as well as the conduction of stimuli by nerve cells. Thus, changes in the conformation and /or structure of molecules that are responsible for the cell attachment to the implants surface, like calcium-binding proteins [5], are to be envisaged. It is therefore of critical importance to get a better understanding of the electrochemical behaviour of metallic implants both after mechanical disruption of the passive film and of the stability of the protecting oxide film when exposed to physiological solutions.

This work describes the results concerning the stability of the passive film on cp titanium, Ti6Al4V, Ti6Al7Nb and CoCrMo implant alloys in serum bovine as well as the repassivation rate after mechanical disruption of the passive film (fretting). The influence of the surface treatment (mechanically polished or sandblasted) is also addressed.

## EXPERIMENTAL

Commercial pure (cp) titanium, Ti6Al4V, Ti6Al7Nb and CoCrMo (67% Co, 28% Cr, 6% Mo) both mechanically polished to 1 µm diamond paste and sandblasted (200 – 500 µm alumina particles) were used for the electrochemical tests. Electrolytes used were calf serum bovine at pH 7.0 and 4.0 and 0.1M sodium sulphate; pH 4.0 was reached by adding hydrochloric acid. The stability of the passive films over time (expressed by the polarization resistance) was determined using electrochemical impedance spectroscopy (EIS).

The repassivation behaviour [6] was studied measuring the open circuit potential before, during and after mechanical disruption of the passive film in serum.

## RESULTS AND DISCUSSION

*Stability of the passive film*

The polarization resistance Rp and thus the stability of the passive film of TiAlV is highest both when sandblasted (fig. 1b) and mechanically polished (fig. 1a). The stability of the passive film is found to be higher in serum bovine compared to 0.1M sodium sulphate solutions, hence, the interaction with biological molecules leads to a general increase in the stability of the sample. This might be due to the formation of an organic adsorption layer which covers part of the electrodes or hinders ion transport.

From the comparison between fig. 1a and 1b it ensues that the sandblasting process improves the stabiliy of the oxide films both in sodium sulphate and in serum. In contrast to mechanically polished samples which have a thin, freshly formed oxide film, sandblasted electrodes are already covered by a stable oxide film originated during the surface treatment and aged through long exposure to air. Thus, changes after immersion are less pronounced.

*Fretting and Repassivation*

The corrosion currents of the implant materials tested during fretting (in the active state) in serum bovine at pH 4 and 7 are very high, indicating that, under fretting condition, the change in the chemical composition of the electrolyte might be significant. The CoCrMo alloy shows – especially at pH 7 – the lowest dissolution currents.

It is crucial that, when passive films are mechanically damaged, the current produced as a consequence of the repassivation processes and the time requested to rebuild a stable passive film are as low as possible. The repassivation rate after fretting was determined by observing the increase in the open circuit potential of the electrodes. The values of the percentage given in fig. 2b is calculated from the potential measured 30 seconds after the end of fretting and referred to the potential reached after 1 hour of repassivation. As can be observed, the two titanium implants behave similarly at pH 7 whereas the CoCrMo alloy shows a very slow repassivation at pH 4.

## CONCLUSIONS

The interaction with serum leads to an increased stability against general corrosion of both mechanically polished and sandblasted samples compared to sodium sulfate solutions.

On mechanically polished samples the thickness of the oxide film increases after exposure to the electrolytes. Hence, the resulting passive film is slightly less stable compared to sandblasted samples of the same composition.

Titanium and Ti6Al4V repassivate with the same velocity and develop the same current in the active state.

CoCrMo alloy at pH 7.0 shows the lowest corrosion current and the highest repassivation rate. However, a decrease of the pH down to 4.0, due to local acidification, renders the cobalt-based alloy worse than titanium and titanium-alloy.

## REFERENCES


[1] Metals Handbook, ninth edition, volume 13 Corrosion, 1987.

[2] L.M.Rabbe; J. Rieu; A. Lopez, P. Combrade, *Clinical Materials*,15, 221-226, 1994.

[3] R.M. Hall, A. Unsworth, Biomaterials, 18, 1017-1026, 1997.

[4] M.A.Khan, R.L. Williams, D.F.Williams, *Biomaterials* 20, 765-772, 1999.

[5] Jan Eirik Ellingsen, *Biomaterials*, 12, 593-596, 1991.

[6] Assi F. Tribolelectrochemistry at a Micrometer Scale, Dissertation at the Swiss Federal Institute of Technology, 2000.


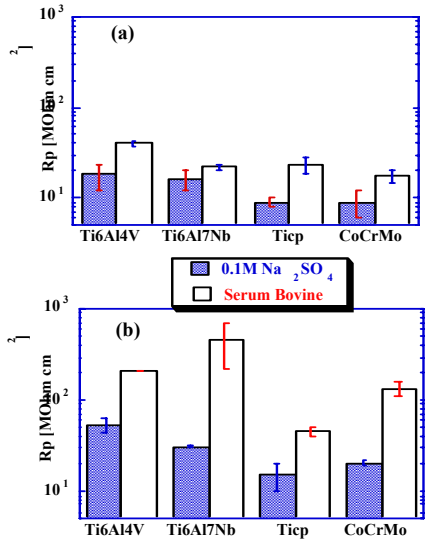


*Figure 1: Effect of the electrolyte and sample composition on the steady state polarization resistance of mechenically polished (a) and sandblasted samples (b).*

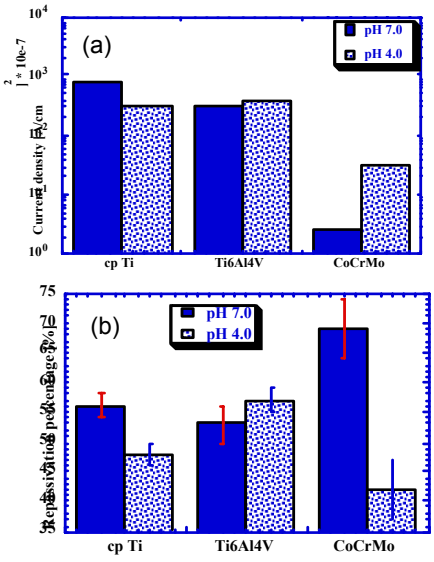


*Figure 2: Effect of pH and sample composition on the corrosion current in the active state in serum. (a) and on the repassivation rate in serum (b).*

European Cells and Materials Vol. 1. Suppl. 1, 2001 (pages 16-17) ISSN 1473-2262

# STIFFNESS OF VITAL-AVITAL COMPOSITE IS INCREASED BY MECHANICAL STIMULATION

K. Alberti[1, 2], G. Raeber[1], E. Karamuk[1], G. Ettel[1], E. Wintermantel[3] and J. Mayer[1]

*[1]Biocompatible Materials Science and Engineering, Swiss Federal Institute of Technology, Zurich, Switzerland, [2]Humboldt University, Berlin, Germany, [3]Zentralinstitut für Medizintechnik der TU München, Germany*

**INTRODUCTION:** Tissue engineering offers the possibility of replacing damaged tendons and ligaments by the means of functional vital/avital composites that consist of a biodegradable matrix and autologous cells[1]. Mechanical stimuli represent one of several concepts to induce differentiation of vital/avital composites towards functional tissues[2]. The aim of this study was to investigate the effects of cyclic mechanical stimulation on a vital/avital composite that consists of a woven fabric as a scaffold and confluent fibroblasts as a vital matrix. The response to mechanical stimulation was evaluated by force measurement, fluorescence staining of the cytosceleton and SEM analysis.

**METHODS:** The vital/avital composite consisted of a textile cell carrier which was seeded with 3T3 fibroblasts at a density of 600cells/mm$^2$ and harvested for two weeks on a shaker at normal cell culture conditions. The poly(ethyleneterephtalat) (PET) monofilament mesh (mesh opening 190 µm, filament diameter 36 µm) was subjected to a temper procedure and $O_2$- plasma activation prior to seeding in order to reduce residual stresses in the textile and increase hydrophility.

The matured composites were installed in the six strain modules of the TissueTens apparatus[3] with the filament axis at a 45° angle with respect to the direction of the uniaxial stimulation and subjected to a 2% sinusoidal stretch. Each stimulation cycle comprised a 1 hour exertion followed by a 6 hour recreation phase where the composites were stimulated at 0,5Hz and 0,01Hz, respectively. A Mesh without cells but otherwise identically treated was used as a reference.

Piezoelectric sensors monitored continuously the stiffness of the composites until they were removed from the strain modules after up to 12 stimulation cycles and prepared for Rhodamin-Phalloidin, Ethidiumbromid-/FDA and DNA staining (Hoechst 33258) as well as for SEM analysis.

The orientation of f-actin filaments with respect to the local strains within single meshes of the textile cell carrier was quantitatively determined by analyzing CLSM image stacks with an autocorrelation algorithm.

**RESULTS:** The stiffness of the vital/avital composites increased during each exertion phase compared to the reference. The subsequent relaxation phase lead to a stiffness reduction. However, there was considerable memory effect leading to an overall gain in stiffness (*Fig.1*). F–actin filaments of samples taken in the middle of the exertion phase were aligned to a high degree parallel to the orientation of the main strains. The recreation phase induced a reorganization of the cytoskeleton, and caused a more random f-actin filament distribution as seen by image analysis (*Fig.2*).

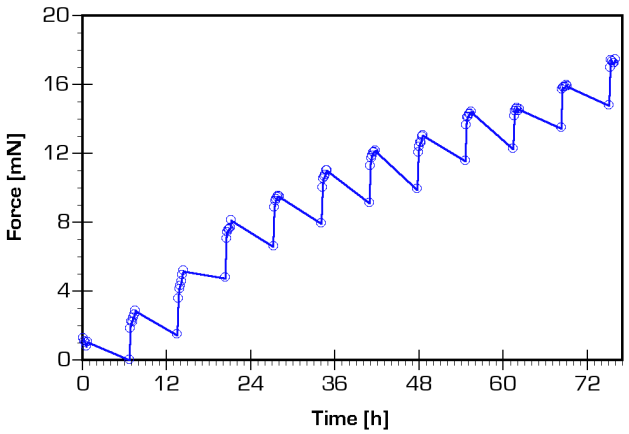


*Fig. 1: Effect of uniaxial mechanical stimulation on the stiffness of vital/avital composites. In contrast to the stiffening of the composite throughout the exertion phase, stimulation at 0.01Hz during recreation caused an increase of the compliance.*

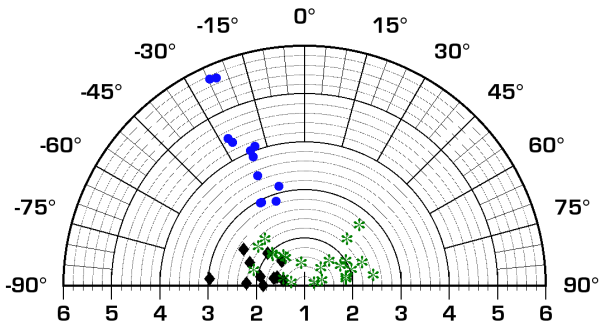


*Fig. 2: Polar diagram of f-actin orientation. Radius: Degree of orientation, Angle: Direction of f-actin filaments (• cells during stimulation, ♦ cells during recreation, ∗ unstimulated cells)*

**DISCUSSION & CONCLUSIONS:** Our experimental setup allowed a continuous force monitoring with a resolution of $5 \cdot 10^{-5}$ N and showed a time-dependent increase of stiffness of the vital/avital composite during mechanical stimulation, which could be correlated with the spatial orientation of f-actin in the cytoskeleton. The response of the f-actin polymerization/depolymerization mechanism was depending on the stimulation frequency. During the exertion phase at 0.5 Hz f-actin fibers were mainly oriented parallel to the external strains whereas at low frequencies (0.01 Hz) the fibers were distributed more randomly. Unstimulated cells showed an orientation distribution close to uniform. These findings suggest that in the concept of tensional homeostasis[4] the intended endogenous matrix tension is depending on the stimulation frequency.

The reason for the overall increase of stiffness has yet to be identified. Possible effects are an increase of cell mass or the deposition of ECM, e.g. collagen type I. A fibroblast cell line was chosen for these experiments because of it's well defined phenotype. However, our next experiments will focus on primary tenocytes on partially degradable textile scaffolds to investigate the balance between ECM formation and scaffold degradation in combination with cyclic mechanical stimulation.

**REFERENCES:**

[1]V.S. Lin, M.C. Lee, S. O'Neal et al (1999), *Tissue Engineering*, **5** (5):443-451.

[2]F. Goulet, D. Rancourt, L. Germain et al. in *Principles of Tissue Engineering, 2nd Edition* (2000).

[3]A. Bruinink, D. Siragusano, G. Ettel, et al (2001) *Biomaterials,* in press.

[4]R.A. Brown, R. Prajapati, D.A. McGrouther et al (1998) *J.Cell.Physiol.* **175**:323-332.

European Cells and Materials Vol. 1. Suppl. 1, 2001 (pages 18-19) ISSN 1473-2262

# SURFACE MODIFICATION OF PVC ENDOTRACHEAL TUBES: OXYGEN PLASMA TREATMENT AND AGING EFFECTS

D. Balazs[1], D. Favez[1], Y. Chevolot[1], N. Xanthopoulos[1],
C. Granges[2], B.-O. Aronsson[2], F. Sidouni[2], P. Descouts[2] and H. J. Mathieu[1]

[1] *Materials Science & Engineering Dept., EPF Lausanne,*
[2] *Group of Applied Physics-Biomedical, University of Geneva*

**INTRODUCTION:** Nosocomial pneumonia is a major medical problem which causes high mortality in intubated and mechanically ventilated patients. A study involving 4500 infected intensive care patients from all over Europe, demonstrated that *Pseudomonas aeruginosa* is one of the most important Gram-negative pathogens, responsible for 30% of nosocomial infections [1]. Colonization of the intubation device and the trachea by *P. aeruginosa* occurs in over 90% of ventilator-associated pneumonia (VAP), with a mortality exceeding 60% despite aggressive antibiotic therapy. Bacteria and material will interact through physico/chemical interactions at the surface of the material. It is through 1) comprehension of these interactions 2) and modification of the material's surface that one may control biofilm formation. Therefore, a new approach is sought to reduce the incidence of *P. aeruginosa* VAP. In the following paper, surface modification with oxygen plasma is investigated as a possible solution. We present ATR-FTIR, XPS and contact angle data pertaining to the surface chemistry of our native and oxygen-modified tubes.

**METHODS:** Control samples were 1cm$^2$ sections cut from Mallinckrodt Medical endotracheal tubes. These samples were then modified with an oxygen glow discharge plasma[2] excited by a direct current (DC) with a voltage of 2 kV, and a gas pressure of 20 Pa. Samples were treated for varying exposition times, including 60 s and 120 s.

For contact angles a water drop of 3.0 µl was deposited on the surface and imaged with a CCD on an optical microscope. The left and right side angles between the water droplet and the surface were then measured. The standard error made with this method is estimated to be ±5°.

XPS analysis was performed using a Kratos AXIS hemispherical analyser with a monochromatic Al $K_\alpha$ x-ray source.

ATR-FTIR measurements were done on a Perkin-Elmer infra red spectrometer equipped with a Goldengate total reflection diamond crystal. 64 spectra in the range 4500-500cm$^{-1}$ are recorded with a resolution of 1cm$^{-1}$ and averaged.

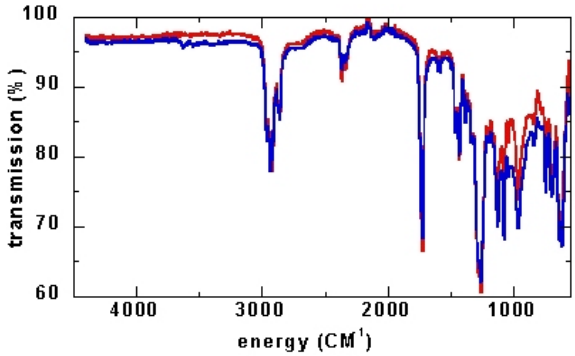


*Fig. 1: ATR-FTIR spectra of native PVC (red) and $O_2$ plasma modified PVC (blue), demonstrating that plasma modification does not alter the bulk material.*

**RESULTS:** The ATR-FTIR analysis demonstrates that oxygen plasma treatment does not alter chemical composition of the bulk material when compared to the native control (*Figure 1*). This was confirmed for various exposure times (60 s, 120 s, and 240 s; data not shown).

*Figure 2* shows the deconvolution of the C 1s peak for native PVC and a sample which had been exposed to an $O_2$ plasma for 120 s. The figure

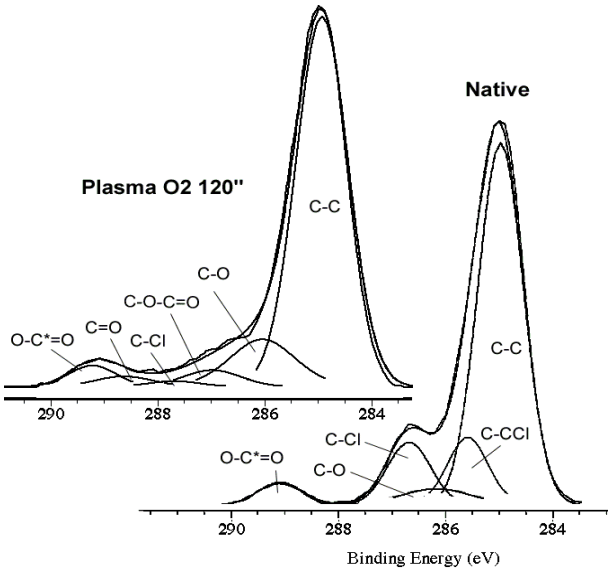


*Fig. 2: Deconvolution of C 1s peak for both native (right) and $O_2$ plasma modified PVC (left), showing the dechlorination of the plasma-modified sample, as well as an increase in oxygenated functional groups.*

demonstrates an increase in oxygenated functional groups, with the creation of carbonyl groups (3% for $O_2$ plasma, 0 % for native) as well as 4-fold increase in the quantity of the C-O contribution (*Table 1*). The C 1s deconvolution also shows a dechlorination, as the C-Cl contribution of the plasma modified sample decreases to 0.8 % from the 9.0 % value of the native sample (*Table 1)*

Another interesting observation with XPS lies in the detection of O-Fe contribution in the O1s peak for the plasma modified sample (figure not shown). This contribution appears because the anode used in the plasma apparatus is composed of stainless steel.

Contact angle measurements demonstrate a sharp increase in hydrophilicity of $O_2$ plasma-modified PVC, compared to native samples. After 120 s of exposure to the oxygen glow discharge the contact angle decreases to 20 $\pm$ 5°, whereas the native sample yields a value of 77 $\pm$ 5 °.

*Table 1. Relative quantities of different functional groups present in native PVC and $O_2$ plasma-modified PVC, after XPS analysis*

| | C-C | C-O | C=O | O=C-O | C-Cl | O-Fe | Zn-Cl |
|---|---|---|---|---|---|---|---|
| Native | 82.3 | 3.8 | 0.0 | 3.8 | 8.9 | 0.0 | 1.3 |
| $O_2$ Plasma | 75.0 | 12.6 | 3.1 | 4.9 | 0.8 | 2.6 | 1.0 |

**DISCUSSION & CONCLUSIONS:** The three aforementioned techniques, ATR-FTIR, XPS, and contact angle permit the characterization of native and of $O_2$ plasma-modified PVC, at varying depths from the surface. ATR-FTIR, the least surface sensitive of the three techniques, demonstrates that there is essentially no modification of the bulk material following oxygen plasma treatment, as expected. XPS permits the analysis of the chemical composition of the first 10 nm of the surface. This method demonstrates that $O_2$ plasma-modification does indeed yield an incorporation of oxygenated functional groups, which should in turn increase the surface wettability[3]. XPS also demonstrates a dechlorination following plasma treatment. Finally, contact angle measurements, the most surface sensitive, demonstrate that the exposure to the oxygen glow discharge greatly increases the surface wettability, yielding a highly hydrophilic surface (<20° $\pm$5°).

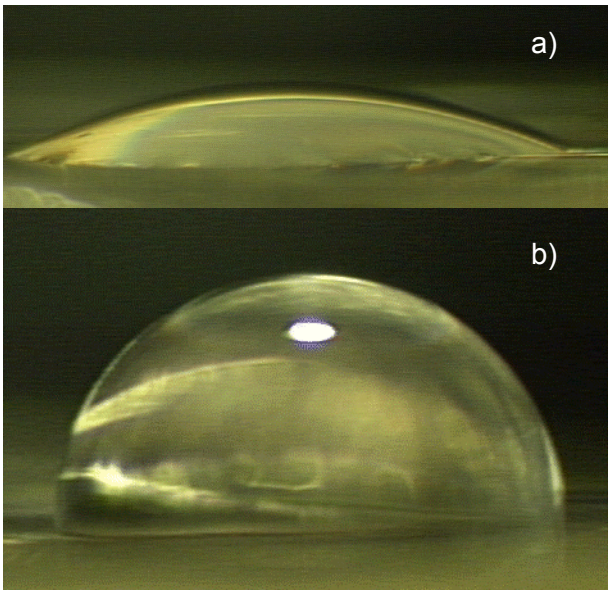


*Figure 3. Water interaction on a) $O_2$-plasma treated PVC and b) native PVC. Angles are about 20° and 77°, respectively.*

**REFERENCES:**

1 J. L. Vincent, D. J. Bihari, P. M. Suter et al (1995) *JAMA* **274**: 639-644

2 B.-O. Aronsson, J. Lausmaa, and B. Kasemo*, J. Biomed. Mater. Res.* (1997) **35:** 49-73.

3 N. Inagaki, *Plasma surface modification and plasma polymerization*. (1996)

**ACKNOWLEDGEMENTS:**

We greatly acknowledge the financial support of the Common Program on Biomedical Engineering and Research, University of Geneva and EPFL, (1999-2002)

European Cells and Materials Vol. 1. Suppl. 1, 2001 (pages 20-21) ISSN 1473-2262

# IMMEDIATE IMPLANTATION OF TITANIUM DENTAL IMPLANTS ASSOCIATED TO AN INJECTABLE BONE SUBSTITUTE IMMEDIATELY AFTER TOOTH EXTRACTION

D Boix[1,2], O. Gauthier[1,3], JM. Bouler[1], P Weiss[1], G Grimandi[1], J Guicheux[1], JL Ardouin[2], G Daculsi[1].

*[1]INSERM 99-03 Research centre on materials of biological interest,Nantes, France [2]School of dental surgery, Nantes, France [3]National veterinary school, Nantes, France.*

**INTRODUCTION:** Two surgical techniques are currently used for placing dental implants. On one hand, implantation may be performed 4 or 6 months after the tooth extraction when alveolar bone healing is achieved. On the other hand, immediate implantation may also be performed allowing a faster prosthetic restoration. With regards to the various morphology of the receiver bone site, which rarely allows immediate implantation, the differed surgical protocol is mostly used. In this context, the use of bone substitution materials associated to dental implantation could allow to perform immediate implantation more frequently. In the present work, we investigated for the first time bone regeneration around dental implants placed immediately in extraction sites in association of a new injectable bone substitute (IBS).

**METHODS:** IBS consisted in a suspension of a mineral phase in a polymeric carrier. The mineral phase was a biphasic calcium phosphate (BCP) with a 60/40 HA/ß-TCP weight ratio. The carrier was a 2 % hydroxypropylmethylcellulose gel (HPMC) in water. Animal experiments were performed on 3 Beagle dogs. Each third and fourth mandibular premolars were extracted. A 5-mm-height bone defect was created at the mesial side of the socket before receiving 10-mm-long, 3,3-mm-diameter titanium implants (*Esthetic plus* TPS, Straumann ITI, Waldenburg, CH). In left sites, IBS was injected in bone defects to cover the mesial exposed part of implants (Fig 1). The right defects were not filled. Animals were sacrificed 3 months later. Implants were observed in scanning electron microscopy (Fig 2). Bone-to-implant contact (BIC) and peri-implant bone density (PBD) were evaluated using a semi-automatic image analyzer (Quantimeter 500, Leica, cambridge, UK).

**RESULTS:** BIC was superior in the sites filled with IBS as compared to the control sites (48% ±12 vs 38% ±12). Furthermore, BIC observed in the filled defects was not significantly different from that observed in the distal side of the socket where no defect was created (48% ±12 vs 49% ±10,5). Similar results were observed with the PBD measurement (44 % ±11 in mesial control site, 58,5% ± 13 in mesial filled defect and 59,5% ±13 in distal sites).

*Fig 1: Injection of IBS around dental implant into the bone defect.*

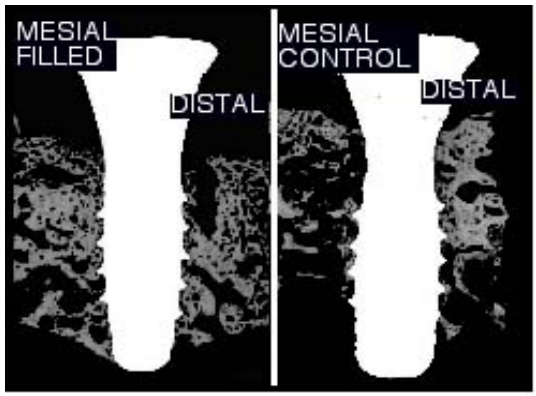


*Fig 2. Bone regeneration around dental implant into filled socket (left) and control sites (right)*

**DISCUSSION & CONCLUSIONS:** Our results strongly suggest that IBS used as a reconstructive material in case of bone damages improve the bone regeneration around titanium dental implants. The development of IBS in dental implantology may favour the use of immediate surgical procedure which in turn may reduce the time necessary for prosthetic rehabilitation.

**ACKNOWLEDGEMENTS:** The authors wish to thank the Straumann Institute for providing us dental implant.

# The Microtensile Bond Strength Test :

## New insight into the performance of adhesive resins bonded to dental substrates

S Bouillaguet [1] T Genovese [2], M Cattani[1], Ch. Godin[1] and JM Meyer[1]

[1] *Division of Biomaterials, School of Dental Medecine, University of Geneva, Geneva Switzerland,*

[2] *Private practice, St Imier, Switzerland*

### INTRODUCTION

Many laboratories use simple shear or tensile bond tests to evaluate the bonding performance of adhesive systems to dental substrates. However, with modern adhesives, there is an increasing incidence of cohesive failures in dental tissues during testing. The microtensile bond strength test (MTBS test) allows the testing of very small cross-sectional areas and develops a uniform stress distribution so that most bond failures occur interfacially [1,2]. Through careful trimming of the specimens, this method also permits isolation of specific types of dental tissues in addition to specific locations inside the tooth. The aim of this study was to evaluate the bond strength of an experimental adhesive system to enamel, normal dentin and caries-affected dentin using the microtensile test.

**METHODS:** Human molars were prepared with high speed diamond burs under coolant to expose enamel, dentin and caries-affected dentin surfaces. The adhesive resin (EXP) was applied according to manufacturer's instructions and covered with Z100 composite resin material (3M ESPE). Each specimen was mounted on a low speed saw (Isomet, Buehler Ltd., Lake Bluff, IL) and serially sectioned perpendicular to the bonded surface. The slices widths were trimmed at the bonded interface to reduce the bonded surface area to approximately 1.0 $mm^2$ [3]. The slabs were then glued with cyanoacrylate (Zapit, DVA, Anaheim, CA, USA) on the opposite rods of a custom made holder and stressed at 1mm/min with a V1000,Vitrodyne testing machine (Vitrodyne V-1000, Chatillon, Greensboro, N.C., USA). The tensile bond strength of each slab was calculated as the force at failure divided by the bonded cross-section surface area (MPa).

**RESULTS:** The mean and the standard deviation of the tensile bond strength of EXP to enamel was 18.9 ± 5.3 MPa (n=15). For dentin and caries-affected dentin the results were respectively 25.9 ± 9.05 MPa. and 29.0 ± 9.7 MPa. Whereas the MTBS to enamel was significantly lower compared

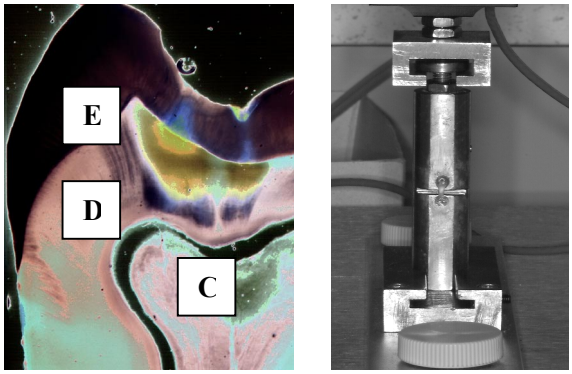


*Fig. 1: The different types of substrates in carious teeth (**E**namel, **D**entin, **C**aries-affected dentin) Fig. 2: The Microtensile testing machine holder with a specimen in place (surface area 1.0 $mm^2$)*

to dentins (P< 0.05), there were no statistical differences between the two dentin groups (P = 0.5242).

**DISCUSSION & CONCLUSIONS:** Adhesive systems have two major functions in restorative dentistry, bonding for retention of composites and sealing of dental substrates. Further, bonding should be as uniform as possible to resist the contraction stresses generated during the polymerization of the restorative material. The use of the microtensile bond strength test allowed us to make comparisons between the performances of this adhesive system applied to clinically relevant substrates. Despite a simplification of the bonding procedures with the EXP adhesive material, the results of this study have indicated that enamel bonding needs to be improved.

### REFERENCES:

[1] Sano H, Shono T, Sonoda H et al. (1994)

*Dent Mater;**10**: 236-40*

[2] Pashley DH, Carvalho RM, Sano H, Nakajima M, Yoshiyama M, Shono Y, Fernandes C, Tay F. (1999) *J. Adhes Dent;**1**: 299-309*

[3] S. Bouillaguet, P. Gysi, B. Ciucchi, M. Cattani, Ch. Godin, J.M. Meyer.(2000) *J. Dent;**29**: 55-63*

**ACKNOWLEDGEMENTS:** This study was supported by 3M ESPE Co. (St Paul, MN, USA)

European Cells and Materials Vol. 1. Suppl. 1, 2001 (pages 23-24) ISSN 1473-2262

# INFLUENCE OF MICROSTRUCTURAL CHANGES OF TITANIA CELL CARRIERS ON HEPATOCYTE PERFORMANCE

S. Buchloh[1], B. Stieger[2], J. Mayer[1]

[1]*ETH Zürich, Inst. for Biocompatible Biomaterials Science and Engineering, Schlieren, Switzerland*

[2]*Div. of Clin. Pharmacol. and Toxicol.,Dep. of Medicine, University Hospital, Zürich, Switzerland*

**INTRODUCTION:** For an Extracorporal Liver Support Device a suitable cell carrier material has to be found. Titanium dioxide ceramics, a biocompatible material, have been demonstrated to be useful as porous cell substrate materials whose properties serve to enhance cell vitality [1]. While other cell types are sensitive to subtle differences in surface roughness and surface chemistry [2] this has not been investigated for hepatocytes. On collagen foams of pore size ranges around 80 µm, hepatocytes exhibited higher albumin secretory activity than on foams in the 18 µm range [3]. In this work the influence of the porosity of a Titania cell carrier material on hepatocyte performance was characterized. Hepatocyte cell number, vitality and activity were determined by protein mass, MTT and NR assays.

**METHODS:** Rutile powders with different grain size distribution have been produced by thermal treatment of a Titaniumdioxid powder (Kronos 1171) and subsequent sieving. These powders were mixed with an organic Binder (PVA 22000, Fluka), unaxially pressed to disks of 20 mm diameter. After sintering the greenbodies up to 1650°C the final porous disks were grinded to their end shape of approximately 15 x 1 mm and polished. Samples were cleaned and steam sterilized at 121°C, 2 bar for 30 min.

Ceramic samples, polished titania single crystals and as positive control poly-vinyl-chlorite (PVC) plates were placed in 24 well plates and seeded with freshly isolated rat hepatocytes [4], using 1 ml Williams Medium E per well, with a cell density of $1*10^6$ cells/ml. For control the tissue culture p

lates poly-styrene (TCPS) was used uncoated and collagen coated (CC TCPS). Samples were incubated at 37 °C for 5 days in a humidefied atmosphere with 5 % $CO_2$. Medium (0.5 ml) was exchanged first after 3 h and then every 24 h. After 5 d, protein mass, MTT (at 560 nm) and NR (at 540 nm) were measured.

**RESULTS:** Measured cell mass for all flat and dense surfaces (Titania ceramic, Titania single crystal, TCPS and PVC) show less total protein then the porous ceramics (Fig. 2). Comparing the dense ceramic (0 µm) and the ceramic with pores around 200 µm, protein mass is doubled on the porous material. In SEM (Fig. 1) it can be seen that the hepatocytes form large agglomerates on, respectively in the pores.

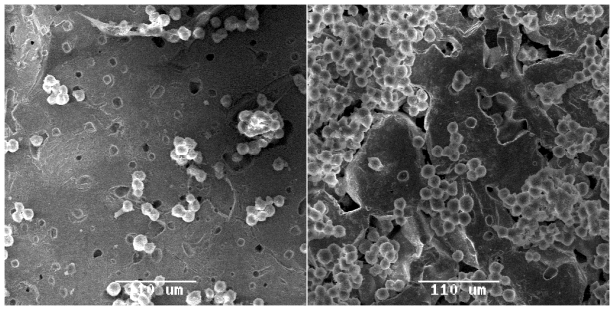


*Fig. 1: SEMicrograph of hepatocytes on Titania ceramics after 5 d. Right: Dense ceramic (0 µm). Left: Porous ceramic (pore size ≈ 200 µm)*

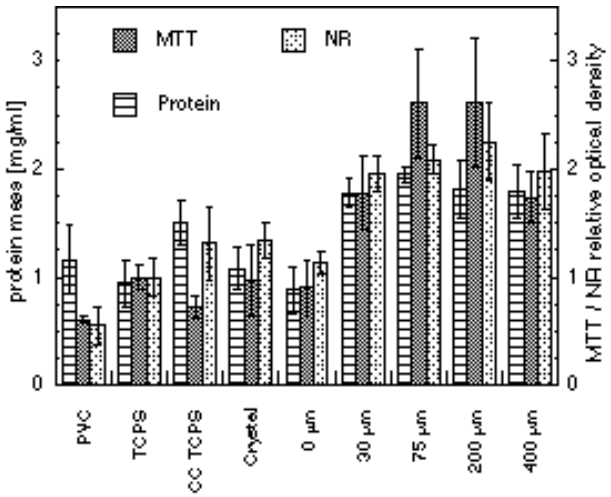


*Fig. 2: Hepatocytes on Titania ceramic after 5 days. Numbers shown give average pore size. (n=6)*

**DISCUSSION & CONCLUSIONS:** For the investigated range of porosities an influence of the pore size on hepatocyte attachment and performance can be found. Possible reasons for this different performance on porous materials of the same composition can be the induced agglomeration as described by Ranucci [3], or a better diffusion of media to the cells. A third possibility is, that the higher available surface leads to higher attachment of hepatocytes.

Hence a possible hepatocyte cell carrier has to be structurally optimized to enhance hepatocytes performance.

**REFERENCES:** [1] K-L. Eckert (1999*) Titania ceramic surfaces as scaffolds for hepatocyte culture* I.C. American Ceramic Society Cocoa Beach. [2] B.D. Boyan (1996) *Role of material surfaces in regulating bone and cartilage cell response* Biomaterials **17**; 137-146. [3] C. Ranucci (2000) *Control of hepatocyte function on collagen foams: sizing matrix pores toward selective induction of 2-D and 3-D cellular morphogenesis* Biomaterials, **21**: 783-793. [4] U. Boelsterli (1995) *Identification and characterization of a basolateral dicarboxylate/cholate antiport system in rat hepatocytes* Am J Physiol, 268: 797-805

**ACKNOWLEDGEMENTS:** I want to thank Ms. Gerspacher for conducting the cell culture experiments.}

European Cells and Materials Vol. 1. Suppl. 1, 2001 (pages 25-26) ISSN 1473-2262

# POLYMERIZATION SHRINKAGE OF ORMOCER BASED DENTAL RESTORATIVE COMPOSITES

M. Cattani-Lorente, S. Bouillaguet, Ch. Godin, and J.M. Meyer

*Dental School, University of Geneva*

**INTRODUCTION:** Resin based dental restorative materials shrink during their setting reaction, which is a radical polymerization. Stresses exercised on the cavity walls during polymerization result in either postoperative sensibility or gap formation at the resin-tooth interface with subsequent bacterial infiltration and secondary caries [1, 2]. Hence, the reduction of the polymerization shrinkage is an actual challenge in the dental restorative field.

New monomers with low volumetric shrinkage have been prepared recently. Multi-methacrylates and highly branched methacrylates were respectively prepared by Culbertson *et al*. [3] and Klee *et al*. [4]. Wolter and Storch [5] proposed the use of ormocers (organic modified ceramics). Ormocers can be depicted as macromonomers with an inorganic silica core grafted with multifunctional methacrylate groups [(poly)alkoxysiloxanes].

The aim of the present study is to measure the polymerization shrinkage of two ormocers and to compare it to the shrinkage of a hybrid and four condensable dental composites. The hypothesis tested is that the use of ormocers effectively reduce the shrinkage of dental restorative materials.

**METHODS:** Two commercially available ormocers (Admira from Voco and Definite from Degussa), a hybrid (Z250 from 3M) and four condensable composites (Solitaire from Heraeus, SureFil from DeTrey, Synergy from Coltene and P60 from 3M) have been used.

The device used to measure the free linear polymerization shrinkage has been validated by Watts and Cash [6]. A disk-shaped unset composite specimen (ϕ:7mm; h:2mm) was placed at the center of a brass ring of 16mm diameter and 2mm height between a rigid glass microscope slide and a glass microscope cover-slip of 0.16mm thickness. A LVDT linear transducer (TESA) was placed on the top of the cover-slip and centrally aligned with the specimen. The polymerization was initiated from below by illuminating the specimen through the rigid glass slide. The polymerization device employed was an ELIPAR Trilight (ESPE). One condition of polymerization only was chosen. The specimen was illuminated for 40 sec with a constant power of 800 mW/cm2.

The shrinkage was measured for 300 sec. Five specimens were measured for each material.

Vickers Hardness was measured with a Hauser indentometer. Five indentations were made by the application of a load of 500 gr. The hardness was measured on the surfaces exposed and unexposed to the light during the polymerization of the same specimens used for the shrinkage determination. The hardness profiles were established by measuring the hardness at different depths. For that purpose, the specimens were first embedded in a resin (Technovit) then cut in half and polished.

**RESULTS:** The mean linear shrinkage values and the filler content with their respective standard deviations are given in Table 1. Mean values marked with the same letter displayed no significant statistical difference using a one way ANOVA followed by a LSD multiple test ($p<0.05$).

*Table 1. Linear shrinkage (%) and filler content (%) of the dental composites.*

| Material | Shrinkage | Filler |
|---|---|---|
| Admira | 1.6 (0.2) c | 0.72 (0.01) b |
| Definite | 1.1 (0.1) b | 0.69 (0.01) b |
| Solitaire | 2.6 (0.2) d | 0.59 (0.02) a |
| Surefil | 0.8 (0.1) a | 0.76 (0.01) c |
| Synergy | 1.8 (0.1) c | 0.70 (0.01) b |
| P60 | 1.0 (0.04) b | 0.79 (0.01) c |
| Z250 | 1.1 (0.1) b | 0.76 (0.02) c |

The Vickers Hardness of the surfaces exposed and unexposed to light are given in the Figure 1.

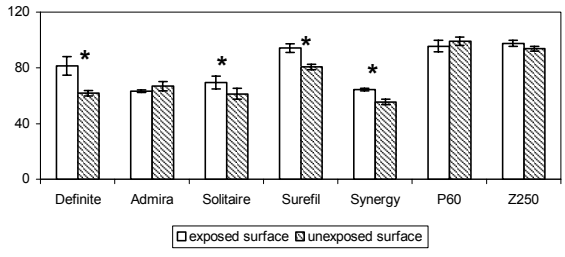


*Fig. 1: Vickers hardness [VHN] of exposed and unexposed surfaces.*

For each composite, values marked with an asterisk are significantly different.

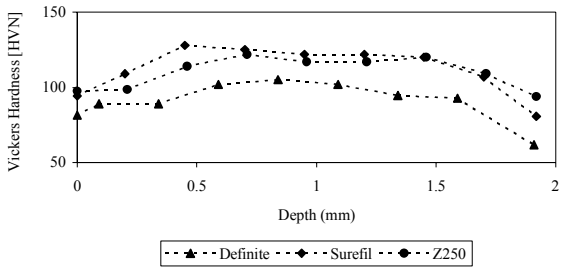


*Fig. 2: Vickers hardness [VHN] profiles. On the x ordinate axis, the zero point corresponds to the light exposed surface.*

**DISCUSSION & CONCLUSIONS:**. The shrinkage of dental composites can be related to their resin content, the chemical nature of the resin, the degree of conversion (DC) from monomers to polymers and the conditions used for the polymerization initiation. In the present study, the later was minimized by using the same source of light, illumination time conditions and temperature.

There is a good linear correlation (r=0.99) between the shrinkage of five composites and their filler content (Figure 3). This probably means that for those materials the quantity of resin is the determinant factor influencing the shrinkage. Based on their respective filler content, a higher shrinkage should be expected for Definite and Surefil. The lower values observed may be due to differences in the chemical composition of their resins.

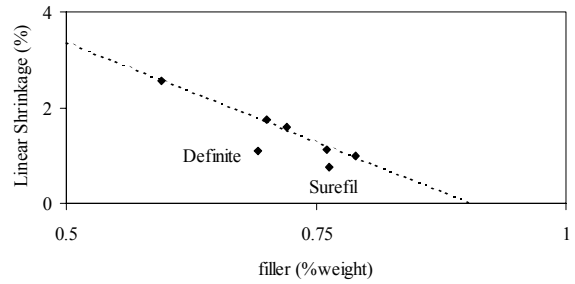


Fig. 3: Correlation between the linear shrinkage and the filler content of the composites.

Surefil is a urethane modified BisGMA resin blended with an irregular shape inorganic filler. These interlocking particles were designed to produce a compact composite with handling characteristics comparable to that of amalgams. It is possible that the interlock of filler particles reduced the shrinkage during polymerization. Provided that the lower shrinkage of Definite is due to the presence of the ormocer, this effect is not observed for Admira, the other ormocer-based composite. There are some differences in the chemical composition of the grafted organic molecules. For instance, functional pending groups of the polysiloxane are methacrylates for Definite. Whereas for Admira there are also carboxylic functions, which do not participate to the radical polymerization. Besides, classical dimethacrylates (Bis-GMA; UDMA; TEGDMA) are present in the two composites to control their viscosity and handling properties. The presence of those monomers can also affect the polymerization shrinkage.

It is often considered that if the hardness of the surfaces exposed and unexposed to light is similar, the polymerization is efficient. In this study four composites presented differences in hardness between exposed and unexposed surfaces. However, at the surface of composites the inhibition layer due to the presence of oxygen lower the hardness, as can be seen in the Figure 2.

Rueggeberg *et al.* [7] showed that the degree of conversion and the volumetric shrinkage of composites are related. The determination of the DC was not done in the present experience. However, based on the fact that there is a good correlation between increasing hardness and increasing degree of conversion [8], we expected a relationship between hardness and shrinkage. However, a multiple regression analysis of the maximum Vickers hardness in function of the filler content and the linear shrinkage showed that the later parameter is not statistically significant at the 90% or higher confidence level. Nevertheless, Surefil presented a high hardness. Hence a high degree of conversion along with a high crosslinking of the polymeric network should be expected for this composite. In the case of Definite the residual double bonds should be quantified to be certain that the lower shrinkage is not due a low degree of conversion.

**REFERENCES:** [1] AJ De Gee, CL Davidson (1987) *J Dent Res* **66**:1636-1639. [2] A Mehl, R Hickel, KH Kunzelmann (1997) *J Dent* **25**:321-330. [3] BM Culbertson, Q Wan, Y Tong (1997) *J Mater Sci: Pure Appl Chem* **A34**:2405-21. [4] JE Klee, F Neidhart, HJ Flammersheim, R Mülhaupt (1999) *Macromol Chem Phys* **200**:517-523. [5] H Wolter, W Storch (1994) *J Sol-Gel Sci Tech* **2**:93-96. [6] DC Watts, AJ Cash (1991) *Dent Mater* **7**:281-287. [7] F Rueggeberg, K Tamareslvy (1995) *Dent Mater* **11**:265-268. [8] JL Ferracane (1985) *Dent Mater* **1**:11-14

# CONTROLLING *PSEUDOMONAS AERUGINOSA* BIOFILM FORMATION: SURFACE MODIFICATION OF PVC ENDOTRACHEAL TUBES WITH DEXTRAN.

Y. Chevolot[1], H. Gao[2], S. Favre-Bonté[3], K. Triandafillu[4], N. Xanthopoulos[1], J. D. Neuvecelle[1], H. Harms[4], D. Balazs[1], C. Van Delden[3], H. Sigrist[2] and H. J. Mathieu[1]

*1 Department of Material Science, EPFL, 1015 Lausanne-EPFL*

*2 CSEM, Jaquet Droz 1, 2007 Neuchâtel*

*3 Department of Genetic and Microbiology, C.M.U., 1 rue Michel-Servet, CH-1211 Genève 4*

*4 Department of Rural Engineering, EPFL, 1015 Lausanne-EPFL.*

**INTRODUCTION**: Data from 4500 infected intensive care patients all over Europe demonstrate that *Pseudomonas aeruginosa* remains the most important Gram-negative pathogen responsible for 30% of nosocomial infections, of which 47% are pneumonia[1]. Intubation with an endotracheal device is the greatest risk factor for pneumonia. Colonisation of the intubation device and the trachea by *P. aeruginosa* occurs in over 90% of ventilator-associated pneumonia (VAP); mortality due to *P. aeruginosa* VAP exceeds 60% despite aggressive antibiotic therapy. Therefore, new approaches must be sought to reduce the incidence of *P. aeruginosa* VAP. The surface was modified with a layer having passivation properties. Dextran [2, 3] is known to have such properties. Optodex® (CSEM) is a diazirine-containing derivative of dextran. Upon light activation, a reactive carbene is generated and can react with the surface and form a covalent bond.

**METHODS** Optodex® was deposited (aqueous solution), dried under vacuum and immobilised by light activation at 350 nm. The samples were washed 3 times in KSCN 3 M, 3 times in PBS/Tween, 3 times in PBS, and finally 3 times in bi-distilled water (5 min sonication for each step). Bacterial adhesion tests were performed in PBS.

**RESULTS:** Dextran binding to PVC was confirmed by XPS analysis (Figure 1).

The washing procedure removed adsorbed molecules. Minimum amounts of Fluorine were detected only on sample C and can also be related to the presence of Optodex®.

Bacterial adhesion was reduced by a factor of 1.4 between sample A and sample C when incubated in PBS.

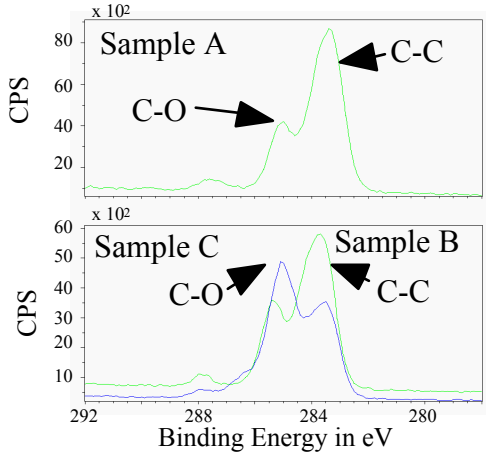


*Fig. 1: XPS C1s of samples A, B and C. Sample A is the pristine surface, B is the surface on which Optodex® was deposited and washed without light activation and C is the surface on which Optodex® was deposited, light activated and washed.*

**CONCLUSIONS:** The chemical treatment was efficient in reducing *P.aeruginosa* adhesion to medical grade PVC.

**REFERENCES:** [1] JAMA 274, 639-644, 1995, [2] Z. Zdanowski, B. Koul, E. Hallberg (1997), J. Biomater. Sci. Polymer Edn, **8**, 825-32. [3] E. Östergerg, K. Bergström, K. Holmberg, et al (1995) *JMBR* **29**:741-77.

**ACKNOWLEDGEMENTS:** The Common Program on Biomedical Engineering and Research (1999-2002), EPFL Lausanne, is greatly acknowledged for financial support.

# INFLUENCE OF SUBCRITICAL CARBON DIOXIDE ON BIODEGRADABLE POLYMERS

F. Maspero[1], K. Ruffieux [1,2], E. Wintermantel[1]

*[1] Biocompatible Materials Science and Engineering, ETH-Zürich, Wagistrasse 23, CH-8952 Schlieren, [2] Degradable Solutions AG, Wagistrasse 23, CH-8952 Schlieren, [3] Zentralinstitut für Medizintechnik der TU München, Boltzmannstrasse 15, D-85748 Garchin*

**INTRODUCTION:** Gaseous carbon dioxide in the subcritical region (T=21°C, P=0-60 bar) can be used as plasticizer or solvent for biodegradable polymers like polylactide and poly(lactide-co-glycolide). Due to its high solubility and its good diffusivity, gaseous carbon dioxide has been applied as physical foaming agent [1], to reduce the processing temperature for injection molding [2] and for manufacturing of open porous structures [3]. Thanks to its biocompatible character, traces of sorbed carbon dioxide present in the polymer matrix do not have to be removed by later purification steps before implantation.

This communication presents the characterization of the solubility and the diffusion kinetics of subcritical carbon dioxide in two different poly(lactide-co-glycolide) copolymer. The influence of the sorbed $CO_2$ molecules on the chemical structure of the polymers and on the glass transition temperature are discussed. Finally, some potential applications for gaseous $CO_2$ in the field of scaffold preparation are presented.

**METHODS:** For the characterization of the subcritical $CO_2$-polymer system, poly(d,l-lactide-co-glycolide) (PLGA 85:15 and PLGA 50:50) plates (thickness: 150-450µm) were used. Sorption isotherm experiments were performed using a high-pressure microbalance. Chemical structure of macromolecules exposed to subcritical $CO_2$ was investigated with FTIR spectroscopy. Phase transitions of the polymers were characterized using differential scanning calorimetry (DSC).

**RESULTS, DISCUSSION & CONCLUSIONS:** Fundamental $CO_2$ anti-symmetric stretch vibrations absorption band at 2340 cm-1, as well as absorption bands at 3590 and 3700 cm-1, also attributed to $CO_2$ vibrations, are visible on FTIR spectra for samples containing sorbed $CO_2$ molecules. Gravimetric measurements carried out simultaneously to FTIR measurements permit to find a correlation between the intensity of the absorption bands and the weight fraction of sorbed $CO_2$. As $CO_2$ molecules desorb, the intensity of the bands decreases. After complete desorption, the entire FTIR spectra are similar to spectra of polymer non-exposed to $CO_2$. This fact tends to confirm that no irreversible process occurs during the sorption.

DSC measurements on PLGA 85:15 and PLGA 50:50 permit to determine the influence of sorbed molecules on the glass transition temperature Tg. As the weight fraction of $CO_2$ in the polymer increases, Tg decreases. During sorption isotherm experiments between 20bar and 55bar, the glass transition temperatures of both PLGA 50:50 (Tg: 55°C) and PLGA 85:15 (Tg: 59°C) drop below room temperature. The experimental results can be fitted with the Flory's model for sorption isotherm of rubbery polymers. Diffusion coefficients have been found to depend on the PLGA composition.

The knowledge about the diffusion coefficient and of the dependency of Tg on the $CO_2$ weight ratio allows optimization of $CO_2$-processing of degradable polymers. As potential application of CO2-processing, the manufacturing of carriers for drug release system will be shown.

**REFERENCES:** [1] Mooney D.J. et al., Biomaterials, 1996, 17(14), 1417-1422. [2] Seibt S.,Thesis, Institut für Kunstoffverarbeitung an der RWTH Aachen, 1996 [3] Maspero F., et al. Proceedings of the 6th World Biomaterials Congress, 2000, Hawaii, USA.

European Cells and Materials Vol. 1. Suppl. 1, 2001 (pages 29-30) ISSN 1473-2262

# CORROSION BEHAVIOR OF METALLIC SURGICAL IMPLANT REX 734 - CoCr ; PITTING, CREVICE AND GALVANIC CORROSION EVALUATION

**L. Reclaru [1], R. Lerf [2], P.-Y. Eschler [1], J.-M. Meyer [3]**

*[1] PX TECH, La Chaux-de-Fonds, Switzerland, [2] PI Precision Implants AG, Aarau, Switzerland, [3] School of Dentistry, University of Geneva, Switzerland*

**INTRODUCTION** The corrosion behavior of combinations of materials used in orthopedic implant REX 734 stainless steel and CoCr alloy has been investigated. This couple of alloys is quite often used in hip prosthesis, were a ball head of CoCr is tapered inter operatively on a hip stem made of REX 734 steel.

The resistance against pitting or crevice corrosion of two alloys REX 734 and CoCr was evaluated according to the standard ASTM F746-87 (re-approved 1994). The galvanic corrosion of coupled REX / CoCr was evaluated by the direct measurement of the corrosion current of the couple and by prediction of the galvanic current using mixed potential theories and potentiodynamic polarization curves (ASTM G71-81).

**MATERIALS** and **METHODS:** Nominal compositions in % weight of the alloys studied are

a) CoCr alloy ISO 5832-12: C 0.085, N 0.15, Cr 27.5, Mo 6.20, Mn 0.7, Si 0.75, Fe < 0.65, Ni < 0.85, Co balance, and

b) REX 734 steel ISO 5832-9: Nb 0.25-0.8, N 0.25-0.5, Cr 19.5-22, Mo 2-3, Mn 2-4.25, Ni 9-11, Si max 0.75, C max 0.08, S max 0.01, P max 0.025, Cu max 0.25, Fe balance.

***a) Pitting and crevice corrosion evaluation :*** The samples for the REX 734 were cut from an orthopedic prosthesis; the samples for CoCr were taken from a bar of diameter 8 mm. The samples were not subjected to any special treatment such as heat treatment, hot or cold working, or passivation treatment. The surface of sample cylinders were metallographically polished with 600-grit paper. The collar used to create the crevice was machined from polytetrafluoroethylene of medical devices purity. The total exposed surface area $A_T$ of the specimen before placement of the collar was 168.8 $mm^2$. The crevice area $A_C$ (area on the internal surface of the collar) was 39.3 $mm^2$.

***b) Galvanic corrosion evaluation :*** The test samples were in the form of small discs (diam. 8 mm), connected to a central stem in order to establish the electrical contact. They were metallographically polished with diamond paste (2 μm). The ratio of anode surface to the cathode surface was equal to one.

***Test milieu:*** 9 g/l NaCl in de-ionized water (18 MΩ.cm); temperature 37° ± 1°C. The pH before and after the test was 5.7 ± 0.2.

***Test equipment***: the electrochemical setup was controlled by an EG&G PAR model 273A in autoexecute running experiments Model 352/252 SoftCorr II (*EG&G Instruments*). The current versus time in the galvanic coupling measurement was controlled by an EG&G PAR model 273A potentiostat, which was modified according to the supplier's instructions to be used as a zero resistance ammeter. This modification permitted measurements of the current variation down to 100 pA.

**RESULTS:**

***a) Crevice and pitting corrosion:*** From the analysis of electrochemical parameters measured and the optical examination of the surfaces below the collar we deduce the pitting or crevice potentials to be 450 mV vs. SCE for the CoCr alloy and, respectively, 500 mV vs. SCE for the REX 734. The REX 734 specimen showed traces of corrosion below the collar. The CoCr alloy revealed a discoloration of the surface.

***b) Galvanic corrosion :*** The coupled REX 734 / CoCr materials exhibit negligible galvanism ; the current generated by the galvanic cell remained low (of the order of nA). There is no risk of triggering the phenomenon of crevice corrosion (crevice potential of the alloys : 450 and 500 mV SCE and couple potential : 10 mV SCE). The values of $i_{couple}$ and $E_{couple}$ were calculated according to the mixed potential theory. The data for predicting galvanic parameters from potentiodynamic polarization curves for REX 734 steel and CoCr alloy (by rotating electrode technique) are also very low (of the order of nA).

**DISCUSSION & CONCLUSIONS:** Table 1 summarizes the results of the galvanic coupling as obtained by the various measurement techniques. All the different techniques lead to the same conclusion that the galvanic currents (whether measured or calculated) are low.

*Table 1. Summary of electrochemical parameters, galvanic current and potential coupling.*

| Techniques, Methods | $E_{couple\ corr}$ | $i_{couple\ corr}$ |
|---|---|---|
| | *mV SCE* | *nA/cm²* |
| Direct measurement | -110 | 6.50 |
| Application of the mixed potential theory | +21 | 32.64 |
| Polarization curves; (fix electrode) | -237 | 96.62 |
| Polarization curves; rotating electrode | -211 | 24.13.36 |

With 500 mV for the CoCr and 450 mV for REX 734, the crevice potential of both materials examined are very high. In consequence, there is no risk for a crevice corrosion caused or amplified by the galvanic coupling.

European Cells and Materials Vol. 1. Suppl. 1, 2001 (page 31) ISSN 1473-2262

# CONFOCAL LASER SCANNING MICROSCOPY (CLSM): A NEW TOOL FOR THE VISUALIZATION OF THE TISSUE IMPLANT INTERFACE.

R. Suetterlin[2], M. Duerrenberger[3], A. Hefti[3], M. Imholz[1], H. Schiel[1], and W. Baschong[1,2]

*[1]Klinik f. zahnärztl. Chirurgie, Zentrum für Zahnmedizin, Univ.Basel; Switzerland, [2] M. E. Müller Institut für Strukturbiologie am Biozentrum, [3] Interdepartementelle Mikroskopie am Biozentrum der Universität, Klingelbergstrasse 50/70, CH-4056 Basel, Switzerland*

**INTRODUCTION:** Microscopic inspection of failed implants are an unique source of direct histological evidence for implant performance eventually leading to improved implant design and to treatment changes beneficial to implant success (1, 2). Investigated are either ground sections of methyl-metacrylate-embedded implants: At the cellular level by histologic analysis of the peri-implant tissue by light microscopy, or at the supramolecular level by transmission electron microscopy (TEM). Alternatively, the tissue/ implant interface is visualized by scanning electron microscopy (SEM). The two approaches exclude each other because of the invasiveness of sample preparation.
In complementation, we elaborated conditions for the non-invasive subcellular analysis of the tissue/ implant interface by confocal laser scanning microscopy (CLSM), and for subsequent analysis by SEM.

**METHODS:** *In vitro*: Human fibroblasts were seeded onto Ti-disks (Ø 1 cm) with machine polished (MP), sandblasted/ acid etched (SA), titanium plasma-sputtered (TPS), hydroxyl apa-tite-coated (HA) surfaces, and grown to half-confluency. Cells were permeabilized, glutaral-dehyde-fixed and labeled for F-actin by TRITC-phalloidin. *Ex vivo*: Ti-step cylinders were retrieved from patients due to loosening upon othodontic loading, Ti-step screws for infection-related fibrosis. Retrieved implants were stored in 10% formaldehyde. For labeling they were transferred to modified Hanks' buffer pH 6.5 (MHB) permeabilized and fixed essentially as above, and subsequently labeled.
*CLSM:* In vitro samples were viewed as mounted specimen, ex vivo specimen in buffer using water immersible objectives.
SEM: Fluorescently labeled specimen were subsequently dehydrated in graded alcohol and critical point dried for SEM. The plain
metal surface was visualized after removing adhering tissue and the gold layer by sonication /sodium hypochlorite. For details see 3, 4.

**RESULTS:** Least-invasive methods were elaborated for labeling the tissue-implant interface by immuno-fluorescence. CLSM in solution was used to identify subcellular structures and to document its architecture. Subsequent analysis by SEM revealed the surface of the same tissue and upon tissue removal that of the respective metal surface.

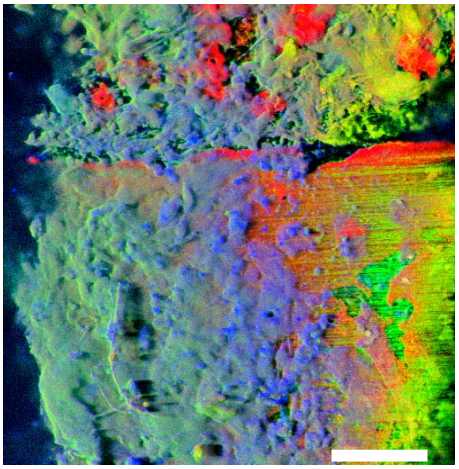

Fig. 1: Fluorescence CLSM image of a Ti-step cylinder, retrieved upon loosening due to orthodontic loading. The smooth part protruded into the oral cavity, the rough TPS-region was anchored in the palatal bone. Triple-labeled for filamentous actin (red); for fibronectin (blue) and for smooth muscle (sm)-alpha-actin (red). Overlay of composite images (75 x 1 µm optical sections). Bar: 100µm.

**DISCUSSION & CONCLUSIONS:** CLSM can be used for documenting the tissue/ implant interface at a subcellular level. The restriction of processing time for labeling and microscopy to 15-18h proved important to control fluorescence fading. Visualization in buffer using water immersion objective lenses was essential for subsequent analysis by SEM.

**REFERENCES:** [1]Steflik, D. E. et al 1991. Intern. J. Oral and Maxillof. Implants 1991. 147-153. [2]Duyck, J., and Naert, I. 1998. Clin. Oral Invest. 2. 102-114. [3]Baschong W. et al. (1999) *Methods in Enzymology* 307. 173-189. [4]Baschong, W. et al. (2001) Micron 32. 33-41

**ACKNOWLEDGEMENTS:** We are indepted to Dr. L. Landmann for letting us use his CLSM facilities and to G. Dorne (Leica Switzl.) for subletting us the water immersion objective lenses for this study. This work was sponsored by the M.E. Foundation and by the Canton of Basel-Stadt.

European Cells and Materials Vol. 1. Suppl. 1, 2001 (pages 32-33) ISSN 1473-2262

# The use of a bioresorbable calcium phosphate cement in partial tibial plateau defects in sheep

Felix Theiss[1], D. Apelt[1],M. Bohner[2], S. Matter[3], Christian Frei[3], J. Auer[1], B. von Rechenberg[1]
[1]MSRU, Dept. of Veterinary Surgery, University of Zurich, Winterthurerstr. 260, CH-8057 Zurich
[2]RMS Foundation, Bischmattstrasse 12, CH-2544 Bettlach
[3]STRATEC Medical, Eimattstrasse 3, CH-4436 Oberdorf

## Introduction

Synthetic bone replacements have been introduced in orthopaedic surgery in various formulations[1,7] with some of them based on natural sources, such as pretreated bovine bone matrix[2], or on synthetic source like hydroxyappatite[3] and tricalcium phosphates[12]. However, liquid bone cements that harden *in situ* and may be shaped according to the wishes of the surgeon are still quite rare. Hydaulic calcium phosphate cements (CPC) were recently described[5,6,9]. The end-product of the reaction is either brushite ($CaHPO_4 \cdot 2H_2O$) or an apatite (e.g. hydroxyapatite $Ca_5(PO_4)OH$) . Based on their solubility, brushite CPC are supposed to be far more resorbable than apatite cements. Several *in vivo* studies have shown indeed that brushite CPC are resorbable[5,6].

In this study, the behavior of two brushite cements was compared to a commercially available apatite cement in an experimental animal model in sheep.

## Materials and Methods

The two brushite CPC (BC1[1] and BC3) were obtained from Dr h.c. Robert Mathys Foundation and Stratec Medical (Switzerland). These CPC are biphasic, i.e. they consist of fine brushite crystals and large granules of β-tricalcium phosphate (β-TCP; <0.5mm in diameter). The porosity of the matrix and the granules is close to 35%. BC1 has the same composition as BC3, except that it contains a larger β-TCP to monocalcium phosphate monohydrate ratio (2 instead of 1.27, in weight percent). The powder-to-granule ratio and the powder-to-liquid ratio are both equal to 2 (in weight percent). The liquid phase consists of a sodium hyaluronate solution.

A partial tibial plateau defect of 2.5 cm in depth and 1 cm heights at the anterior aspect of the tibial crest and an 8 mm drill defect in the distal femoral condyle was used as an experimental model in sheep. 16 sheep were divided in groups A and B. In group A , BC1 was used for the partial tibial plateau defect, whereas BC3 was applied in the drill hole of the femoral condyle. The tibial defect was stabilized by means of a 3.5 mm T-plate with screws. Animals were sacrificed 2, 4, 6 and 8 weeks, and 2, 4 and 6 months after surgery. Group B received a commercially available hydroxyapatite cement (Norian SRS, Norian Corporation, Cupertino, CA, USA) in both, the tibial and the femoral bone defects and served as controls. There, the animals were sacrificed 6 months after surgery.Radiographs were made immediately postoperatively and microradiographs at the time of sacrifice. The bones were harvested immediately after euthanasia. Macroscopic appearance of the defects was recorded, emphasizing tissue reaction of the environment, incorporation of the cement and if possible, the degree of cement resorption and new bone formation. Thereafter histology sections of undecalcified bone samples were prepared[4,8,11], where bone samples were embedded in acrylic resin. Grinding sections of 30-40 µm (Leitz Saw Microtome 1600) and thin sections of 5 µ stained with Toluidine blue or van Kossa/McNeal allowed microscopic analysis where cement resorption, new bone formation and cellular reaction were assessed. Histomorphometrical measurements (Leica, Qwin, Quips Program) were used to calculate the ratio of cement/ new bone according to the time of sacrifice.

## Results and Discussion

Both types of CPC were well integrated within the original defect. The BC1 and BC3 were almost completely resorbed 6 months after surgery. In contrast, almost no bone resorption of the hydroxyapatite cement (Norian SRS) was visible at the same time period. At 2 months, about 25%, and at 4 months about 60% of the BC1 and BC3 was resorbed, while at the resorption front new bone formation was recorded. Although radiologically a small radiolucent zone could be demonstrated in some of the specimens, macroscopically and histologically this gap was not visible. Macroscopically, the cement seemed well incorporated at the bone periphery and no tissue reaction immediately adjacent to the bone cement was noted. Histologically, active bone resorption was demonstrated with osteoclasts directly at the cement surface digesting the original cement material. In the small interface between the new bone and the cement, multinuclear cells with incorporated cement material were seen, while new osteoid was deposited in the surface of TCP granules. TCP granules and the liquid cement phase were replaced by *creeping substitution*[10], which is the normal mechanism of bone replacement.

## Conclusions

Overall, the brushite bone cements were well tolerated by the tissue, and resorbed much faster compared to the hydroxyapatite cement.

## Acknowledgement

Mathys Medical (Bettlach, Switzerland) and Stratec Medical (Oberdorf, Switzerland) are thanked for their financial support.

[1]Under the project name "chronOS Inject" at Mathys Medical and "Cement X" at Stratec Medical

**References**


1. Aebi M. Biologischer oder artifizieller Knochenersatz? In: A. H. Huggler and E. H. Kuner, eds. *Aktueller Stand beim Knochenersatz*. Chur und Freiburg: Springer Verlag Berlin Heidelberg New York, 1991;1-9.

2. Bereiter H, Melcher GA, Gautier E, et al. Erfahrungen mit Bio-Oss, einem bovinen Apatit, bei verschiedenen klinischen Indikationsbereichen In: A. H. Huggler and E. H. Kuner, eds. *Aktueller Stand beim Knochenersatz*. Chur und Freiburg: Springer Verlag Berlin Heidelberg New York, 1991;117-125.

3. Damien CJ, Parsons JR, Benedict JJ, et al. Investigation of a Hydroxyapatite and Calcium Sulfate Composite Supplemented with an Osteoinductive Factor. *J Biomed Mat Res* 1990;24:639-654.

4. Engelhardt P, Gasser JA. LEICA HistoDur: A Resin Specifically Designed for the Histology of Mineralized Tissues. *Leica Applications Brief*. Switzerland: Sandoz Pharma LTD, Osteoporosis Research, 4002 Basel, 1995.

5. Flautre B, Delecourt C, Blary M-C, et al. Volume Effect on Biological Properties of a Calcium Phosphate Hydraulic Cement: Experimental Study in Sheep. *Bone* 1999;25, Supplement:355-395.

6. Ikenaga M, Hardouin P, Lemaitre J, et al. Biomechanical Characterization of a Biodegradable Calcium Phosphate Hydraulic Cement: A Comparison with Porous Biphasic Calcium Phosphate Ceramics. *J Biomed Mat Res* 1998;40:139-144.

7. Kenley RA, Yim K, Abrams J, et al. Biotechnology and Bone Graft Substitutes. *Pharm Res* 1993;10:1393-1401.

8. Leutenegger CM, Rechenberg Bv, Zlinsky K, et al. Quantitative Real Time PCR for Equine Cytokines in Nondecalcified Bone Tissue Embedded in Methyl Methacrylate. *Calcif Tissue Int* 1999;65:437-444.

9. Lu JX, About I, Stephan G, et al. Histological and Biomechanical Studies of Two Bone Colonizable Cements in Rabbits. *Bone* 1999;25, Supplement:415-455.

10. Phemister D. The fate of transplanted bone and regenerative power of various constituents. *Surg Gynecol Obstet* 1914;19:303-333.

11. Rechenberg Bv, Leutenegger CM, Zlinszky K, et al. mRNA of interleukin-1 and 6 are upregulated in subchondral cystic lesions in four horses. *Equine Vet J* 2000;accepted, 2000.

12. Rose PL, Auer JA, Hulse D, et al. Effect of B-Tricalcium Phosphate in Surgically Created Subchondral Bone Defects in Male Horses. *Am J Vet Res* 1988;49:417-424.

# SYSTEMIC SPREAD OF TITANIUM WEAR DEBRIS: TARGET IDENTIFICATION IN A RABBIT MODEL

[1]N. Villinger, [1]M.A. Wimmer, [2]J. Kunze, [1]J. Goldhahn

*[1]AO Research Institute, Davos, Switzerland, [2]Technical University Hamburg-Harburg, Germany*

**INTRODUCTION:** Local effects of wear debris, leading to osteolysis and aseptic loosening, are frequently reported in the literature. While much knowledge has been gained about the local reactions, relatively little is known concerning the dissemination of wear debris beyond the periprosthetic tissues and the systemic reactions. Wear particles, phagocytosed by macrophages, may enter the lymphatic system or may use hematogenous pathways. As shown by a recent study (1), wear particles were detected in the para-aortic lymph node, liver and spleen of patients studied post mortem. The aim of the present study was the identification of target organs and the analysis of histopathological responses to wear debris in affected organs using a rabbit model.

**METHODS:** Titanium wear particles with known characteristics (mean diameter 0.63 µm), were used to produce an overload of wear particles in a bony cavity (8mm depth, 2,5mm diameter), close to the knee joint of a rabbit. The drilling direction was parallel to the joint line. After insertion of the wear debris the drill hole was covered with a periostal flap. Skin closure was performed using non-resorbable materials.

Seven rabbits were operated by the same surgeon, randomized right/left to filled/empty defect. All animals were sacrificed after 16 weeks. Six health rabbits taken from stock underwent euthanasia and served to establish baseline values for metal concentration measurements in tissues.

The spleen, liver, left and right kidney, and the lymph nodes of the right and left femur were removed and cut into half. Metal concentrations of the moieties were determined using inductively coupled plasma – optical emission spectroscopy (ICP-OES) with a limit of determination of 2ng/mg titanium in freeze-dried tissue. The remaining, non-lyophilized organ samples as well as the femoral condyles of the left and right knee were fixed in formalin and embedded in paraffin and PMMA respectively. Microtome sections (6µm) were prepared. The femoral condyles as well as the soft tissue samples were colored using three different staining techniques: hematoxylin and eosin, Perl´s Prussian Blue and alcian blue. All specimens were examined by light microscopy, up to 1000x magnification.

**RESULTS:** After 16 weeks, wear debris was still present inside the insertion location. No signs of inflammation or necrosis could be detected. Particles were also found in the surroundings, encapsulated in the fibrous tissue. The spleen of all experimental rabbits exhibited titanium concentrations above the limit of determination (Tab.1), while no titanium was detected in the spleen of the untreated rabbits. Also, for any animal, all other organ samples displayed concentration values below 2 ng/mg.

| | Animals | | | | | | |
|---|---|---|---|---|---|---|---|
| | 1 | 2 | 3 | 4 | 5 | 6 | 7 |
| Ti (ng/mg) | 3.16 | 4.94 | 9.78 | 5.67 | 2.83 | 5.66 | 3.04 |

Table 1: Titanium concentration in the spleen

Opaque particles were identified histologically in sections of the spleen. The particles appeared dark brown to black. The foreign material was either encapsulated in vacuolated macrophages or accumulated near trabeculae of the spleen. No cellular response as for example granulomous inflammation, fibrosis or necrosis could be detected. No particles were identified in other investigated organs and the lymph nodes.

**DISCUSSION & CONCLUSIONS:** Since no wear debris was found in the lymphatic system and in the liver, this study suggests that immediate hematogenous dissemination of wear debris may be an alternative possibility. In all seven rabbits titanium was identified in the spleen using quantitative measures. Although at the present time we are unable to draw further conclusions about the role of the lymphatic system regarding particle transport, the consistency of the findings suggests hematogenous pathways to remote organs as the principle route for early dissimination of wear debris. The macrophages with ingested particles suggest either an active transport from the periprosthetic tissue to the spleen or a local processing. The mild cellular reaction of the spleen is consistent with recent findings in total joint replacement patients (1). Further studies should elucidate the influence of particle size, shape and material composition on the pathway, as well as the long-term systemic cellular reaction.

**REFERENCES:** (1) R.M. Urban et all (2000) *Dissemination of wear particles to the liver, spleen and abdominal lymph nodes of patients with hip or knee replacement*. JBJS 82-A, No.4

European Cells and Materials Vol. 1. Suppl. 1, 2001 (pages 35-36) ISSN 1473-2262

# A PROTEIN-RESISTANT POLYMERIC INTERFACE FOR BIOAFFINITY SENSING

J. Vörös[1], N.P. Huang[1], S.DePaul[1], M. Textor[1], J. A. Hubbell[2], N. D. Spencer[1]

[1] *Laboratory for Surface Science and Technology and the* [2]*Institute of Biomedical Engineering, ETH Zürich, Switzerland*

**INTRODUCTION:** A novel platform technology for tailored interfaces in sensor applications have been developed based on PEG derivatised cationic polymers. These molecules spontaneously assemble on anionic oxides and provide highly protein resistant surfaces. Furthermore, they can be functionalised to improve selectivity and sensitivity in bioaffinity sensing applications. In the model biotin-streptavidin system, a specific sensor response to streptavidin was achieved by the functionalising the metal oxide surface with biotinylated PEG-containing polymer.

Non-specific protein adsorption is a problem that plagues a wide array of biomedical applications such as serum contacting sensors. Protein adsorption often leads to a sensor response that is not analyte specific. Since metal oxides are commonly present in the biosensor applications, a method for measuring only specific target analytes while eliminating non-specific binding on oxides would be an important development in biosensor technology.

A class of materials based on poly(ethylene glycol) (PEG), a hydrophilic polymer with many properties similar to water, has been found to be remarkably resistant to protein adsorption, and many strategies for the immobilisation of PEG onto surfaces have been developed. [1] The polymer, poly (l-lysine)-g-poly(ethylene glycol), consists of a poly(l-lysine) (PLL) backbone that has been grafted with PEG side chains, some of which were biotinilated. The assembly of the polymer film onto the surface is based on the electrostatic interaction of the positively charged polymer backbone and the negatively charged metal oxide surfaces. These properties make this interface design a useful platform for many sensing applications. Among which, the Optical Waveguide Lightmode Spectroscopy (OWLS) technique was chosen because it is an online, direct, lable-less and highly sensitive technique with high throughput capabilities.

**METHODS:** The OWLS technique involves the incoupling of the evanescent field of a He-Ne laser into a planar waveguide which allows for the direct online monitoring of macromolecule adsorption.[2] It is highly sensitive (i.e. ~1ng/cm$^2$) up to a distance of 100 nm above the surface of the waveguide. Furthermore, a measurement time resolution of 3 seconds allows for the study of adsorption kinetics

10mM HEPES (pH 7.4) buffer solution and $SiO_2$-$TiO_2$ waveguides (Microvacuum Ltd, H) were used for all of the experiments. The modified waveguides were prepared in situ by exposing the waveguides to 1 mg/ml polymer solution for twenty minutes in a flow cell apparatus, followed by rinsing with buffer. Then the PLL-g-PEG-biotin modified waveguides were exposed to Control Serum N (human) (Roche, CH) for thirty minutes and then washed in buffer. At the end of the measurement selectivity was tested with 50 μg/ml streptavidin (SIGMA, USA) for 20 minutes followed by a rinse with buffer.

Mass data were calculated from the thickness and refractive index values derived from the mode equations. [2] All OWLS experiments were conducted in a BIOS-I OWLS instrument (ASI AG, CH).

**RESULTS AND DISCUSSION:** The first part of the experiment, shown in Figure 1, demonstrates the protein resistant behaviour of the treated oxide surface.

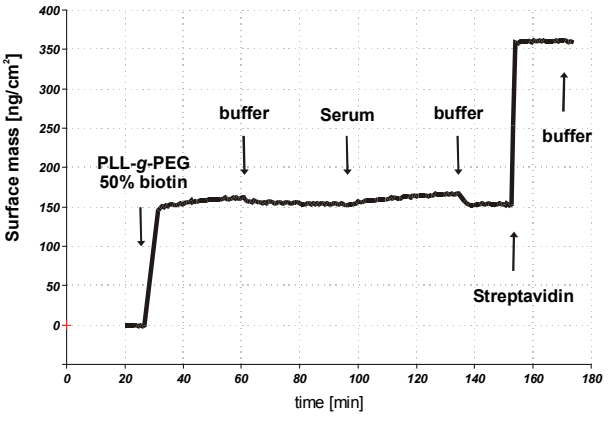


*Fig. 1: Selective sensor response of the biotin derivatised PLL-g-PEG on streptavidin exposure.*

Waveguides coated with the PLL-g-PEG-biotin exhibit protein adsorption of less than 2 ng/cm$^2$ after exposure to human blood serum. This value is two-hundred-fold lower than the adsorption seen on untreated waveguides. The second part of the experiment demonstrates the specificity of the sensor. A monolayer of streptavidin quickly and irreversibly adsorbs onto the same PLL-g-PEG-biotin functionalised surface after exposure to a 50 μg/ml streptavidin solution.

The adsorbed amount of the PLL-g-PEG polymer onto a $SiO_2/TiO_2$ surface depends on the pH and ionic strength of the buffer solution in which it is dissolved. For example, at pH values higher than the pK of the polymer (pK~10) and lower than the isoelectric point of the surface (IEP~4), the mass of adsorbed polymer decreases. Subsequent human serum albumin adsorption experiments at pH 7.4 indicate that the protein resistant property of the PLL-*g*-PEG layer depends on the mass of polymer adsorbed [2].

**REFERENCES:** [1] D. L. Elbert and J. A. Hubbell, *Chemistry and Biology*, **5**(3), 1998, pg. 177-183.

[2] G. L. Kenausis, J. Vörös, D. L. Elbert, N. Huang, R. Hofer, L. Ruiz, M. Textor, J. A. Hubbell, N. D. Spencer, *J. Phys. Chem. B* **104**: 3298-3309*,* 2000.

European Cells and Materials Vol. 1. Suppl. 1, 2001 (pages 37-38) ISSN 1473-2262

# MICROFABRICATED SURFACES TO STUDY CELL-SURFACE INTERACTIONS

M. Winkelmann [1,3], U. Neuwald[1], R. Hauert[2], M. Textor[1] J. Gold[3], N.D. Spencer[1], B. Kasemo[3]
[1] Laboratory for Surface Science and Technology, *ETH Zürich, Zürich, Switzerland*
[2] *Swiss Federal Laboratories for Materials Testing and Research, EMPA, Dübendorf, Switzerland*
[3] *Department of Applied Physics, Chalmers University of Technology, Gothenburg, Sweden*

**INTRODUCTION:** Most artificial materials, once implanted in the patient's body, induce a cascade of reactions with the biological environment through interaction of the biomaterial with body fluid, proteins and various cells. The specific surface interactions determine the attitude the body takes towards the foreign material, the path and speed of the healing process and the long-term development of the biomaterial-body interface. As regards surface properties, both the chemical composition and the topography (structure, morphology) are known or believed to be important in bone, since they regulate type and degree of the interactions that take place at the interface. Microfabrication has proved to be a very valuable tool for producing geometric patterns of well-defined surface chemistry and/or topography. Such surfaces are ideal to study – in separate experiments – the influence of chemical composition and surface morphology and to learn how cells sense surfaces of biomaterials, in both in vitro and in vivo assays.

**MATERIALS AND METHODS:** Silitronix (100)-surface polished silicon 2" wafers were coated with 20nm of either Ti, Al, Nb or V in a thin film deposition system. Wafers were then spin-coated with 1.5mm thick photoresist (Shipley S-1813 Microposit). The samples were exposed to UV light (400 nm; Mercury lamp; 3.5 mWatt/cm$^2$) with a contact printer through a chromium mask. Then developed (Shipley MF322 Microposit) to remove exposed photoresist. A second evaporation with a 20nm layer of either Ti, Al, Nb, or V was carried out. The remaining resist was then removed with acetone. Finally the wafer surface consisted of spatially patterned regions (Figure 1) of Ti, V, Al and Nb, representing models of heterogeneous titanium alloy surfaces currently used in orthopaedic and maxillofacial implants. The dimension of the patterns was varied between 0.5 and 150 mm. Prior to testing and characterizing all samples were cut to 11x9 mm size, extensively washed in acetone-isopropanol-

DI water, treated in an $O_2$-plasma for 5 min and then studied by AFM-LFM, XPS, ToF-SIMS, SAM, SEM and Condensation Figure measurements. Studies of the attachment and spreading behaviour of human osteoblasts on these well defined chemically patterned model surfaces have been carried out in collaboration with University of Nottingham. Further characterizations of the surfaces are currently in progress.

**RESULTS AND DISCUSSIONS:** AFM-LFM: Scans over the edge of the pattern showed sometimes a lip up to 20 nm high. On a Ti/Ti sample the bottom layer roughness had a Rms of 0.56±0.13 nm, though the pattern (top layer) had a 3 fold value of 1.64±0.45 nm.

XPS: The survey spectra showed a low amount of C which indicate that the applied cleaning procedure is ok. Further investigation with the PHI Quantum XPS showed in the well defined reading points the element expected. Line scans showed a sharp change between the patterned regions.

ToF-SIMS: The metal film surfaces have been shown to be protected by natural oxide layers upon exposure to air. The most prominent stoichiometries have been found to be: $TiO_2$, $Al_2O_3$, $V_2O_5$ and $Nb_2O_5$.

SEM: Results indicated a uniform consistent array of events on all of the surfaces. The edges of the pattern are rounded due to the photolithography process.

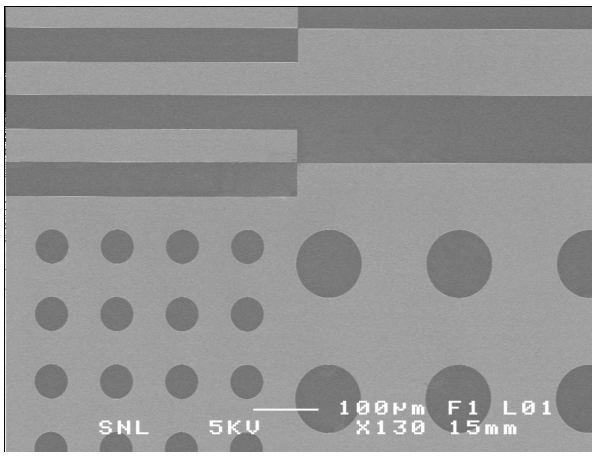

*Fig. 1: The sample layout used had different areas with either stripes or dots in the range of 50, 100, and 150 mm.*

**ACKNOWLEDGEMENTS:** Portions of this research have been sponsored by a fellowship provided by the Swiss National Science Foundation (83EU-054771). Additionally support from Roche Research Foundation and Swedish Biomaterials Consortium is gratefully acknowledged. Samples were made in the Swedish Nanometer Laboratory. Irene Pfund is thanked for the ToF-SIMS measurements.

European Cells and Materials Vol. 1. Suppl. 1, 2001 (pages 39-40) ISSN 1473-2262

# ELECTROCHEMICAL SURFACE TREATMENT OF TITANIUM APPLIED TO BIOLOGICAL MODEL SURFACES

O. Zinger and D. Landolt

*Laboratoire de Métallurgie Chimique, Département des Matériaux,*
*Ecole Polytechnique Fédérale de Lausanne, CH-1015 Lausanne EPFL, Switzerland*

## INTRODUCTION

Titanium and titanium alloys have attracted considerable interest in aerospace, chemical process and biomedical industry due to their biocompatibility, good mechanical properties and excellent corrosion resistance.

The chemical stability of titanium results from the presence of a thin but stable surface oxide film, typically a few nanometer thick. In nonaqueous electrolytes containing perchloric or sulfuric acid, the oxide film is unstable and anodic polarization leads to titanium dissolution at high rate. Recently, a sulfuric acid based-methanol electrolyte has been developed for electrochemical polishing of titanium [1,2]. Best polishing was obtained in an electrolyte containing 3 M sulfuric acid for applied potentials above 8 V corresponding to mass-transport controlled dissolution conditions [2]. Using this electrolyte, well-defined topographies in the micrometer range were produced on bulk titanium by electrochemical micromachining through a patterned photoresist [3]. This method involves high-speed selective metal dissolution from unprotected areas of a photoresist-patterned workpiece that is made an anode in an electrolytic cell. Compared to chemical etching, electro-chemical dissolution offers higher rates and better control on a micro- and macro-scale of shape and surface texture of anodically dissolved materials.

Biological performances of implantable titanium devices in medicine and dentistry have been shown to depend on their surface topography. This latter must be carefully controlled in the micro and nanometer range to achieve cell adhesion and differentiation [4]. Thus, through-mask electro-chemical micromachining appears to be a useful method for the fabrication of well-defined surface structures on bulk titanium**.**

## METHODS

The different steps of the process are shown on Fig. 1. The experimental details are described thereafter.

Commercially pure titanium disks (Ti 99.6%) were mechanically polished to obtain a mirror finish surface. The polished titanium was coated with a negative polyimide based photoresist, which was exposed using a standard UV mask aligner and developed to reveal the initial patterns.

The dissolution of the titanium through the patterned photoresist was performed in a methanol based electropolishing electrolyte with 3 M sulfuric acid [3].

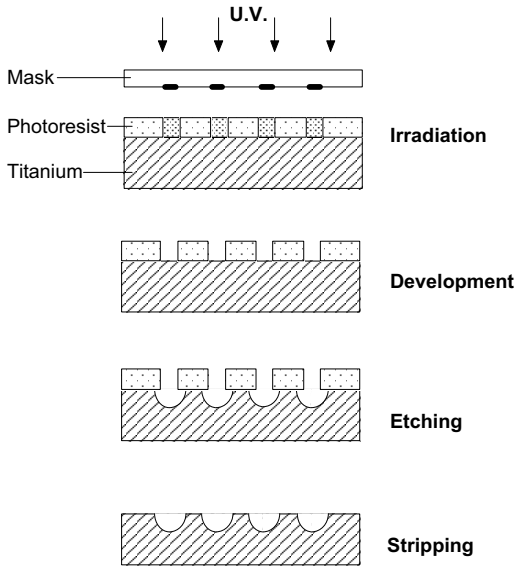


*Fig. 1 Processing steps for through-mask electrochemical micromachining of titanium*

## RESULTS

High dissolution rates can lead to Joule heating, affecting precision of the attack and therefore reproducibility. Joule heating is important for a pattern with a large etched surface area and/or high density. To reduce this effect, the electrolyte is cooled down to –10°C; ethanol was added to the methanol (50/50 mixture) to increase viscosity and decrease the anodic current.

To study the role of the surface topography on the interactions of cells with implants, specific patterns were designed; some of them having a

very high density, still resulting in excessive Joule heating. Fig. 2 shows a hole presenting a bad surface finish coming from an excess of heat.

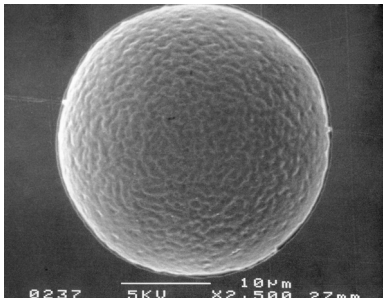

*Fig. 2 SEM micrograph of a hole (∅ 30 µm) dissolved with non-optimized parameters*

To be able to dissolve titanium with smooth surface finish and good reproducibility, a special sample-holder cooled from the inside was developed, and electrochemical parameters were optimized. First, a short polarization of 40 V was applied to remove the titanium oxide as quick as possible to obtain an homogeneous dissolution from the beginning of the process; then, to reduce Joule heating effects, the potential was gradually decreased to 15 V and maintained at this voltage until the end of the dissolution. Fig. 3 presents a 30 µm diameter hole with smooth surface texture and sharp edge obtained under these optimized conditions. Fig. 4 shows an array of the same 30 µm diameter holes in hexagonal compact arrangement. The separation of the holes is 3 µm.

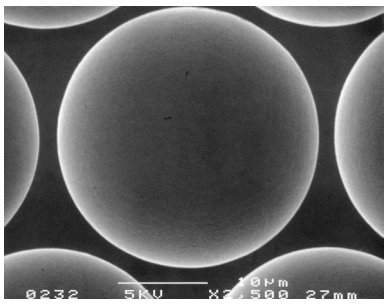

*Fig. 3 SEM micrograph of a hole (∅ 30 µm) dissolved with optimized parameters*

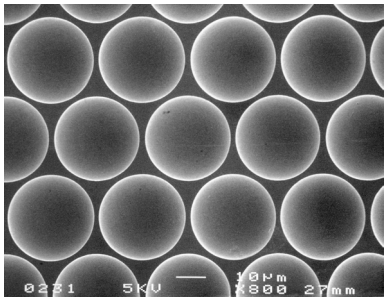

*Fig. 4 SEM micrograph of an array of holes (∅ 30 µm) in hexagonal compact arrangement*

## CONCLUSIONS

The optimization of electro-chemical parameters and the use of a cooled sample-holder enabled us to produce dense and well-defined surface structures in the micrometer range on bulk titanium with smooth surface finish and good reproducibility. These structures will serve as model surfaces to study the role of the surface topography on the interactions of cells with implants.

## REFERENCES

[1] O. Piotrowski, C. Madore, and D. Landolt, *Plat. Surf. Finish.*, **85**, 115 (1998) [2] O. Piotrowski, C. Madore, and D. Landolt, *J. Electrochem. Soc.*, **145**, 2362 (1998) [3] C. Madore, O. Piotrowski and D. Landolt, *J. Electrochem. Soc.*, **146**, 2526 (1999) [4] B. D. Boyan, T. W. Hummert, D. D. Dean and Z. Schwartz, *Biomaterials*, **17**, 137 (1996).

## ACKNOWLEDGEMENTS

The authors thank B. Senior (CIME-EPFL) for the SEM pictures. Financial support of the Commission Fédérale de la Technologie et de l'Innovation (CTI) is gratefully acknowledged.

# TITANIUM AS AN IMPLANT MATERIAL, CLINICAL PERFORMANCE IN NEW TECHNOLOGIES.

Stephan M. Perren

*AO Research Institute and AO development, Davos, Switzerland*

A fracture results in disruption of the continuity of bone stiffness. Bone loses its support function with loss of alignment i.e. loss of anatomical shape. Attempts to use the limb then generate pain and thus functional immobility results.

An implant used for internal fixation of fractures should provide a temporary mechanical scaffold to maintain restored anatomical shape with enough stability to allow free and painless mobility of the injured limb to exercise the soft tissues and thus to avoid the fracture disease. The mechanical requirements regarding the function of an implant material for internal fixation, therefore, are primarily stiffness and strength; both depend on material but even more so on design. In conventional technology the application of the implant requires ductility. The latter allows for shaping of the implant to correspond to the bone shape. In respect to the use of screws the ductility of the implant has an even more important aspect, it protects from overload and failure at application by providing feedback to the surgeon. Titanium is less ductile than steel. If the surgeon using conventional techniques tries to tighten the screws as much as possible failure of Titanium without pre-warning may occur.

The major complications of internal fixation are mechanical failures at implantation, fatigue failures during and after the bone healing and biological failures mainly infection. Today's implant materials are considered to be biocompatible. Still some important differences exist such as different influence on local resistance to infection. Such differences have been ob-served in recent experimental evaluations. The surgeon "knows" that bacterial contamination resulting in infection subsides only when the "foreign" body is removed. Recently the main focus of interest concerned the basic aspects of formation and avoidance of a dead space within an implant and around it. Beside biocompatibility and surface structure tissue strain seems to play an important role in respect to the mechanism of adherence of the soft tissues.

The interaction of surface contact of implants and bone blood supply brought about changes in the philosophy of application and function of the implants. Today a basically different mechanical function of e.g. periosteally ap-plied implants is achieved. These implants now function rather like fixators than like plates with a different mechanical loading of the screws especially at application. As a consequence, commercially pure titanium finds a wider application and offers more advantages than in conventional application. Using the new technology of internal fixation with PC-Fix made of commercially pure titanium out of more than 2000 fixators with an average of more than 5 screw-bolts no screw nor fixator breakage has been observed. It is fascinating to observe how material, de-sign and application interact in the surgical treatment of fractures.

Implants and Infection, S. Arens (Ed.)

AO Scientific Supplement to Injury 27: 1-63 1996

Stephan M. Perren, Surgical aspects of implants and infection, Nova Acta Leopoldina (in press).

# THE INSULT OF A FOREIGN BODY

Samuel G. Steinemann
*Straumann Institute, Waldenburg, & University of Lausanne, Switzerland.*

In living tissue, a surgical implant is a foreign body, which interacts in various manners with its environment. This foreign body can be an insult to life (using a wording of psychiatrist Sigmund Freud in Imago, Bd. 5, 1917) of chemical, physiological or mechanical kind. In fact, this metal implant is not like living tissue, where no free electrons exist and where metals, such as essential trace elements, occur in a bound and not in an elemental state. Any of these interactions between life processes and the implant, i.e. the foreign body, is connected with specific phenomena and a typical length. The bone structure and also for some soft tissue is dependent upon the mechanical environment; these tissues have typical lengths of mm (trabeculae, osteons). Physiological processes, in particular tissue growth, depend upon cells, which have a typical size of micrometers; transport processes in the tissue electrolyte become important. Chemical and physical processes occur in the nanometer range of lengths; over such distances (up to 20nm) can occur the charge transfers of electrons and protons. Adhesion is an example for such processes.

Many laws of biomechanics are known, e.g. for the bending stiffness and bending breaking strength of bone, also Young's modulus and the compressive strength. The question is though: Are the laws of men for prosthetic devices as good as the laws of nature? Three propositions are given: (i) the stiffness of the implant (dental case) should be approximately that for bone, (ii) isoelastic behaviour towards the bone guarantees good load transfer, and (iii) the device should guide and distribute forces and to perform this it must be stiff. Different concepts become apparent, are they wrong or right? Stiffness is the product of two quantities, Young's modulus and the moment of inertia, which varies strongly with size. Young's modulus also varies strongly with the material; the ratio for modulus of material/modulus of bone is 20 for sapphire (Kawahara dental implant), 10 for the cobalt alloy and 5 for titanium (Ti). Material and design of the prosthetic device must match.

Maurer et al (1993) studied cell proliferation (fibroblast, osteoblast) under different conditions: cells are exposed to a metal-saturated electrolyte and grow on an inert support or cells are inoculated and grow on a metal support. The results suggest that the metal-cell interaction has two modes, a weak interaction and a strong interaction. The dissolved metal produces no growth inhibition. Cells must be in contact with the solid metal; then, fibroblasst can proliferate on Ti, Nb, Zr, Ta and osteoblasts can proliferate on Ti, Zr only. This result has high interest.

The connection between bond and implant is amenable to mechanical measurements. The bond can be quantified by push-out and release-torque tests. Their results however depend on surface roughness, i.e. geometry or structure, and may not reflect a functional connection such as adhesion. This latter property is obtained in pull-out tests. The forces to separate an implant from bone are equal to (tensile) strengths up to 3 MPa. This is a high load, which exceeds by orders of magnitude a physical adhesion mechanism such as breaking a vacuum or rupturing Van der Waal's intermolecular bonds. Certainly, there can be no empty space or free water present at the interface. Thus, one may ask: what is the glue? The functional connection, i.e. osseointegration, must hide a chemical origin. Ti is a reactive metal. This means that in air or any aqueous electrolyte, an oxide is spontaneously formed on the metal. Further, as Boehm shows in a classical study, this surface oxide is hydroxylated and has amphoteric, or bipolar character. The chemisorption ability of such surfaces is well known. In particular, peptides and amino acids act as ligands and attach to Ti oxide by replacement of the surface hydroxyl. The kind of bond, however, needs to be specified. A study using X-ray excited photoelectron diffraction of glycine adsorbed on single-crystal rutile shows correct distances and angles among carbon and nitrogen atoms on top of the oxide and this is sufficient evidence for covalent bonding between the amino acid and the (foreign body) oxide. The result of the photoelectron diffraction experiment suggests considering osseointegration on a same footing as peptide formation, i.e. as a condensation reaction. The terminal carboxyl and amino groups of amino acids and proteins bind with the surface hydroxyls. The connecting links of the surface complexes come out to be pieces of the peptide bond, i.e. –(C=O)– and –(N-H)–. Bone adhesion happens in new dimensions.

**References** :S.G. Steinemann in Titanium Science and Technology (Eds.: G. Lütjering, U. Zwicker, W. Bunk), Deutsche Gesellschaft Metallkunde, Oberursel 1985, 1373-1379. A.M. Maurer, V.D. Lê, S.G. Steinemann, H. Guenther, J. Bille, 10th Eur. Conf. Biomaterials, Davos, 1993. H.P. Boehm, Disc. Faraday Soc. 1971, 52, 264-275. L. Pattthey, PhD thesis University of Lausanne, 1995. S.G. Steinemann, Euromat 99, Materials for Medical Engineering (H. Stallforth, P. Revell, eds.)

European Cells and Materials Vol. 1. Suppl. 1, 2001 (pages 41-42) ISSN 1473-2262

# IMPLANT TECHNOLOGY FOR ENDOVASCULAR REPAIR OF CEREBRAL ANEURYSMS: REQUIRED MATERIAL CHARACTERISTICS

O. Jordan[1], K. Barath[2], K. Tokunaga[2], D. Rüfenacht and E. Doelker[1]

*[1]School of Pharmacy, University of Geneva, Switzerland, [2] University Hospital, Neuroradiology, Geneva, Switzerland*

**INTRODUCTION:** Cerebral aneurysms are potentially life-threatening vascular defects. Besides the classical neurosurgical repair of aneurysms using clip devices, endovascular minimally invasive methods have become increasingly accepted alternative treatments for intracranial aneurysms. If feasible, repair of the artery is obtained by excluding the aneurysm from the circulation in order to prevent growth and rupture causing haemorrhage. The purpose of this poster is to present the principal types of aneurysm pathologies, the current endovascular repair strategies, and establishing the list of requirements for current and future implants.

**CEREBRAL ANEURYSM TYPES:** An undue widening of an artery is addressed as aneurysm. Such increase of the lumen may occur due to a focal defect of the arterial wall structures or in relation with a more extensively diseased arterial segment. Such a viewpoint allows for classifying in two basic types of intracranial aneurysms that are either in relation with a **focal wall defect** (e.g. blister-like, saccular aneurysms) or in relation with a **segmental wall disease** (e.g. fusiform aneurysms). The most frequent lesions are saccular aneurysms that typically arise from arterial bifurcation points due to focal defect and grow in relation with hemodynamical stress. They present by haemorrhage, mass effect or incidentally. The small blister-like lesions are rare, and are associated with a focal defect and a very thin wall. Fusiform aneurysms are pathological dilatations of a whole arterial segment and most frequently occur with atherosclerosis. Each aneurysm type requires a specific repair strategy.

**ANEURYSM REPAIR STRATEGIES:** Aneurysmal cavities can be excluded from the circulation by introducing a filling material, what is in the current clinical practice feasible for the repair of saccular aneurysms. The treatment of aneurysms by repair of the arterial wall is a more recent development at the level of cerebral arteries and this involves use of stent devices (endovascular prosthesis), what may be applied for blister-like lesions, fusiform aneurysms, or large necked saccular aneurysm.

**IMPLANT TYPES:** Implants for **filling the aneurysm** are currently mostly metallic coils what allows for a 20-30% filling of the volume of an aneurysm. Such coils form a random network within the aneurysm cavity but are leaving 70-80% of the space filled by clot formation. Overproduction of clot may lead to complication by thromboembolic events, a risk that increases with the size of the focal defect in the arterial wall. On the other hand, clot seals immediately the rupture point and prevents thus re-haemorrhage from happening. However, clot is not permanent and will be resorbed within weeks of time. For a permanent result, tissue repair is required. This is observed in over 90% at follow-up examination in aneurysms treated with coils under the condition that the neck size was smaller than 4 mm. Additional filling implants under development are liquid polymers that polymerise or precipitate when introduced into the cavity. Preformed polymers dissolved in a water-miscible organic solvent allow for a filling of up to 100% of the aneurysm cavity and are currently under clinical evaluation.

Implants for **wall reconstruction** are more difficult to introduce to the cerebral circulation due to the tortuous vascular access route. Early clinical experience shows that the use of endovascular prosthetic material (stent) may be the solution for treating the other types of aneurysms, i.e. blister-like, fusiform and wide necked saccular lesions. Stent porosity and strut size herald the hemodynamical impact and tissue repair induced by such implants.

**GENERAL IMPLANT REQUIREMENTS:** Future progress in endovascular aneurysm treatment will depend largely on implant improvement, including device and delivery system design. Increased safety and simplicity of such procedures will depend on the method and the control of implant application. Visibility and compatibility with modern imaging methods (DSA, CT, MRI) are key characteristics as are the biological and biomechanical properties of an

implant in order to avoid undue thrombus formation and to induce lasting tissue repair.

# HYFRASURF – ADVANCED SURFACE TECHNOLOGY FOR SUPERIOR ELECTRODE PERFORMANCE

Jörg Krumeich, F. Jansen

*Sulzer Markets and Technology Ltd, Sulzer Innotec, Winterthur, Switzerland*

**INTRODUCTION:** In recent years much effort has gone into prolonging the lifetime of batteries in pacemakers. The focus has been mainly on the optimisation of the battery and on a higher integration of the electronic circuits and consequently a lower power consumption. By introducing a modification of the electrode tip it has been possible to reduce power consumption with the potential for further optimisation.

**METHODS:** The HyFraSurf technology (HyFraSurf = Hybrid Fractal Surface Topography) is based on a micro-fractal treatment and coating deposition process (Fig. 1).

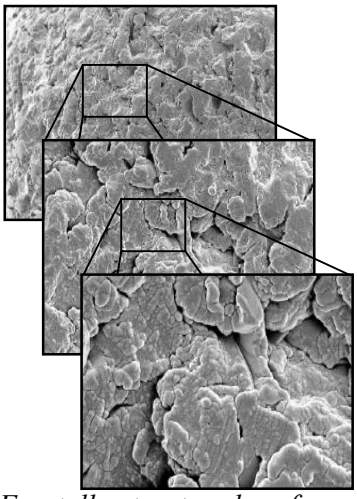

*Fig.1: Fractally structured surface of HyFraSurf-treated electrode tips.*

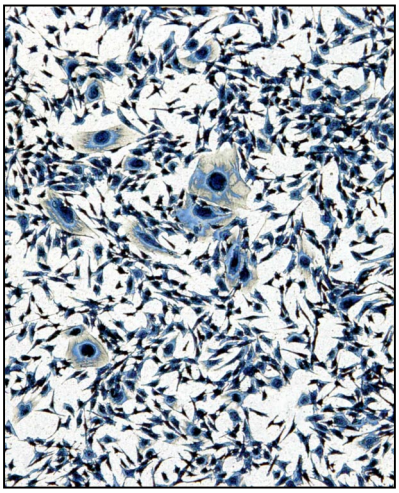

*Fig.2: Polarisation Voltage and Double Layer Capacity of different surface modifications.*

**RESULTS:** Sulzer Innotec has developed a proprietary surface treatment, which has demonstrated higher double layer capacity and lower polarisation voltage. By adapting the process parameters, the modification can be optimised for different requirements (Fig. 2).

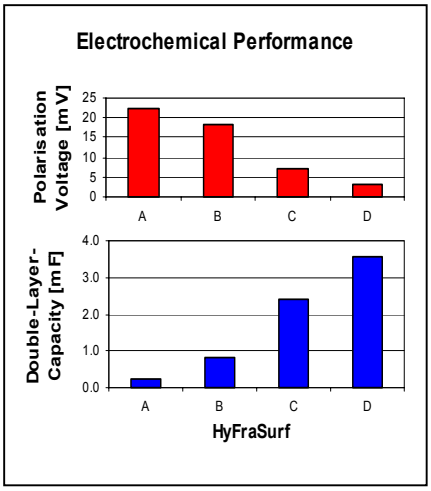


*Fig. 3: In vitro test of bacterial proliferation on HyFraSurf surface modification.*

Biocompatibility was tested in-vitro. The results of the cell culture tests showed good cell coverage (Fig.3). Compared to the untreated reference surface, HyFraSurf demonstrates excellent biocompatibility.

**DISCUSSION & CONCLUSIONS:** For artificial stimulation of the heart, the electrode current, which is carried by electrons, has to be coupled into the tissue, where ions are the main contributors to conductivity. To achieve this coupling effectively it is necessary to create a high double layer capacitance and a low polarisation voltage at the interface. By depositing a highly biocompatible coating displaying a micro-fractal surface topology, the double layer capacity and the polarisation voltage can be influenced. A strong correlation between the increase of the double layer capacity and the decrease of the polarisation voltage is present. Therefore, the electrical resistance of the interface between electrode tip and tissue is significantly reduced. Furthermore, HyFraSurf can be tailored to meet specific electrochemical requirements.

**REFERENCES:** J. Brehme, V. Biehl, A. Hofmann, Adv. Eng. Mat. 2, 2000, 270-275. M. Schaldach, M. Hubmann, M. Hardt, R. Weike, A. Weike, Biomed. Technol. 1989, 185. J. Riedmüller, A. Bolz, H. Rebling, M. Schaldach, Proc. 14th ann. Int. Conf. of the IEEE/EMBS 1992, 2364-2365.